
Robust Inverse Reinforcement Learning under Transition Dynamics Mismatch

Luca Viano
EPFL

luca.viano@epfl.ch

Yu-Ting Huang
EPFL

yu.huang@epfl.ch

Parameswaran Kamalaruban*
LIONS, EPFL

kamalaruban.parameswaran@epfl.ch

Volkan Cevher
LIONS, EPFL

volkan.cevher@epfl.ch

Abstract

We study the inverse reinforcement learning (IRL) problem under the *transition dynamics mismatch* between the expert and the learner. In particular, we consider the Maximum Causal Entropy (MCE) IRL learner model and provide an upper bound on the learner’s performance degradation based on the ℓ_1 -distance between the two transition dynamics of the expert and the learner. Then, by leveraging insights from the Robust RL literature, we propose a robust MCE IRL algorithm, which is a principled approach to help with this mismatch issue. Finally, we empirically demonstrate the stable performance of our algorithm compared to the standard MCE IRL algorithm under transition mismatches in finite MDP problems.

1 Introduction

Recent advances in Reinforcement Learning (RL) [1, 2, 3, 4] have demonstrated impressive performance in games [5, 6], continuous control [7], and robotics [8]. Despite these successes, a broader application of RL in real-world domains is hindered by the difficulty of designing a proper reward function. Inverse Reinforcement Learning (IRL) addresses this issue by inferring a reward function from a given set of demonstrations of the desired behavior [9, 10]. IRL has been extensively studied, and many algorithms have already been proposed [11, 12, 13, 14, 15, 16].

Virtually all IRL algorithms rely on the assumption that the expert demonstrations are collected from the same environment, where the IRL agent is trained. However, this assumption rarely holds in real-world; There is often a mismatch between the learner and the expert’s transition dynamics, resulting in poor performance that are critical in healthcare [17] or autonomous driving [18]. Indeed, the performance degradation of an IRL agent due to transition dynamics mismatch has already been noted empirically [19, 20, 21, 22], but none of these works provide theoretical guidance on this issue.

To this end, our work first provides a theoretical study on the effect of such mismatches in the context of the infinite horizon Maximum Causal Entropy (MCE) IRL framework [23, 24, 25]. Specifically, we bound the potential decrease in the IRL learner’s performance as a function of ℓ_1 -distance between the expert and the learner’s transition dynamics. We then propose a robust variant of the MCE IRL algorithm to recover the reward function under the transition dynamics mismatch effectively.

There is precedence to our robust IRL approach, such as [26] that employs an adversarial training method to learn a robust policy against adversarial changes in the learner’s environment. We

*Corresponding author.

incorporate this idea within our IRL context, by viewing the expert’s transition dynamics as a perturbed version of the learner’s one, and systematically develop our robust MCE IRL algorithm.

Our robust MCE IRL algorithm also leverages techniques from the robust RL literature [27, 28, 29, 26]. Few recent works [19, 20, 30] attempt to infer the expert’s transition dynamics from the demonstration set or via additional information, and then apply the standard IRL method to recover the reward function based on the learned dynamics. Still, the transition dynamics can be estimated only to a certain accuracy level, i.e., we still have a mismatch between the learner’s belief and the dynamics of the expert’s environment. Our robust IRL approach can be incorporated into this research vein to improve the IRL agent’s performance further. In particular, our main contributions are the following:

1. We provide an upper bound for the suboptimality of an IRL learner that receives expert demonstrations from an MDP with different transition dynamics, with respect to (w.r.t.) the one that receives demonstrations from an MDP with the same transition dynamics of the learner environment (*cf.*, Section 3).
2. We find suitable conditions under which a solution to the MCE IRL with a model mismatch optimization problem exists (*cf.*, Section 3.1).
3. We propose a robust variant of the MCE IRL algorithm to learn a policy from expert demonstrations under transition dynamics mismatch (*cf.*, Section 4).
4. We demonstrate our method’s robust performance compared to the standard MCE IRL in a broad set of experiments under both linear and non-linear reward settings (*cf.*, Section 5).

2 Problem Setup

This section formalizes the robust IRL problem. We use bold notation to represent vectors.

Environment and Reward: We formally represent the environment by a Markov decision process (MDP) $M_\theta := \{\mathcal{S}, \mathcal{A}, T, \gamma, P_0, R_\theta\}$, parameterized by $\theta \in \mathbb{R}^d$. The state and action spaces are denoted as \mathcal{S} and \mathcal{A} , respectively. We assume that $|\mathcal{S}|, |\mathcal{A}| < \infty$. $T : \mathcal{S} \times \mathcal{S} \times \mathcal{A} \rightarrow [0, 1]$ represents the transition dynamics, i.e., $T(s'|s, a)$ is the probability of transitioning to state s' by taking action a from state s . The discount factor is given by $\gamma \in (0, 1)$, and P_0 is the initial state distribution. We consider a linear reward function $R_\theta : \mathcal{S} \rightarrow \mathbb{R}$ of the form $R_\theta(s) = \langle \theta, \phi(s) \rangle$, where $\theta \in \mathbb{R}^d$ is the reward parameter, and $\phi : \mathcal{S} \rightarrow \mathbb{R}^d$ is a feature map.

We use one-hot feature map $\phi : \mathcal{S} \rightarrow \{0, 1\}^{|\mathcal{S}|}$, where the s^{th} element of $\phi(s)$ is 1 and 0 elsewhere. Our results can be extended to any general feature map, but we use this particular choice as a running example for concreteness. We focus on state-only reward function since the state-action reward function is not that useful in the robustness context.

We denote an MDP without a reward function by $M = M_\theta \setminus R_\theta = \{\mathcal{S}, \mathcal{A}, T, \gamma, P_0\}$.

Policy and Performance: A policy $\pi : \mathcal{S} \times \mathcal{A} \rightarrow [0, 1]$ is a mapping from a state to a probability distribution over actions. The set of all valid stochastic policies is denoted by $\Pi := \{\pi : \sum_a \pi(a|s) = 1, \forall s \in \mathcal{S}; \pi(a|s) \geq 0, \forall (s, a) \in \mathcal{S} \times \mathcal{A}\}$.

We are interested in two different performance measures of any policy π acting in the MDP M_θ : (i) The total expected return $V_{M_\theta}^\pi := \mathbb{E}[\sum_{t=0}^\infty \gamma^t R_\theta(s_t) \mid \pi, M]$, and (ii) its entropy regularized variant $V_{M_\theta}^{\pi, \text{soft}} := \mathbb{E}[\sum_{t=0}^\infty \gamma^t \{R_\theta(s_t) - \log \pi(a_t|s_t)\} \mid \pi, M]$.

The state occupancy measure of a policy π in the MDP M is defined as $\rho_M^\pi(s) := (1 - \gamma) \sum_{t=0}^\infty \gamma^t \mathbb{P}[S_t = s \mid \pi, M]$, where $\mathbb{P}[S_t = s \mid \pi, M]$ denotes the probability of visiting the state s after t steps by following the policy π in M . Note that $\rho_M^\pi(s)$ does not depend on the reward function. Let $\boldsymbol{\rho}_M^\pi \in \mathbb{R}^{|\mathcal{S}|}$ be a vector whose s^{th} element is $\rho_M^\pi(s)$. For the one-hot feature map ϕ , we have that $V_{M_\theta}^\pi = \frac{1}{1-\gamma} \sum_s \rho_M^\pi(s) R_\theta(s) = \frac{1}{1-\gamma} \langle \theta, \boldsymbol{\rho}_M^\pi \rangle$.

A policy π is *optimal* for the MDP M_θ if $\pi \in \arg \max_{\pi'} V_{M_\theta}^\pi$, and we denote an optimal policy by $\pi_{M_\theta}^*$. Similarly, the *soft-optimal* policy (always unique) in M_θ is defined as $\pi_{M_\theta}^{\text{soft}} := \arg \max_{\pi'} V_{M_\theta}^{\pi', \text{soft}}$ (*cf.*, Appendix B for a parametric form of this policy).

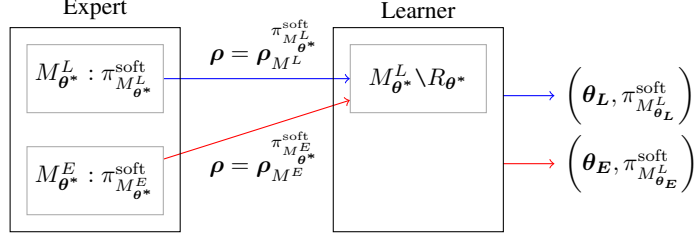


Figure 1: An illustration of the IRL problem under transition dynamics mismatch: See Section 2.

Learner and Expert: In our setting, we have two entities. A learner implementing the MCE IRL algorithm, and an expert. We consider two MDPs $M_{\theta^*}^L = \{\mathcal{S}, \mathcal{A}, T^L, \gamma, P_0, R_{\theta^*}\}$ and $M_{\theta^*}^E = \{\mathcal{S}, \mathcal{A}, T^E, \gamma, P_0, R_{\theta^*}\}$ that differ only in the transition dynamics.

The true reward parameter $\theta = \theta^*$ is known only to the expert. The expert provides demonstrations to the learner: (i) By following policy $\pi_{M_{\theta^*}^E}^{\text{soft}}$ in M^E when there is a *transition dynamics mismatch* between the learner and the expert, or (ii) by following policy $\pi_{M_{\theta^*}^L}^{\text{soft}}$ in M^L otherwise. Note that, similar to [19], we consider a soft-optimal policy for the expert. The learner always operates in the MDP M^L and is not aware of the true reward parameter, i.e., it only has access to $M_{\theta^*}^L \setminus R_{\theta^*}$. It learns a reward parameter θ and the corresponding soft-optimal policy $\pi_{M_{\theta}^L}^{\text{soft}}$, based on the state occupancy

measure ρ it received from the expert. Here, ρ is either $\rho_{M^E}^{\text{soft}}$ or $\rho_{M^L}^{\text{soft}}$ depending on the case. Our results can be extended to estimate ρ via Monte Carlo samples using concentration inequalities [11].

Our learner model builds on the MCE IRL framework that matches the expert’s state occupancy measure ρ . In particular, the learner policy is obtained via solving the following problem:

$$\arg \max_{\pi \in \Pi} \mathbb{E} \left[\sum_{t=0}^{\infty} -\gamma^t \log \pi(a_t | s_t) \mid \pi, M^L \right] \quad (1)$$

$$\text{subject to } \rho = \rho_{M^L}^{\pi} \quad (2)$$

Note that this optimization problem only requires access to $M_{\theta^*}^L \setminus R_{\theta^*}$. The constraint (2) follows from our choice of one-hot feature map. We denote the optimal solution of the above problem by $\pi_{M_{\theta}^L}^{\text{soft}}$

with a corresponding reward parameter: (i) $\theta = \theta_E$, when we use $\rho_{M^E}^{\text{soft}}$ as ρ , or (ii) $\theta = \theta_L$, when we use $\rho_{M^L}^{\text{soft}}$ as ρ . Here, the parameters θ_E and θ_L are obtained by solving the corresponding dual problems of (1)-(2). Finally, we are interested in the performance of the learner policy $\pi_{M_{\theta}^L}^{\text{soft}}$ in the MDP $M_{\theta^*}^L$. Our problem setup is illustrated in Figure 1.

3 MCE IRL under Transition Dynamics Mismatch

This section provides a bound on the MCE IRL learner’s suboptimality when there is a transition dynamics mismatch between the expert and the learner, as compared to an ideal learner without this mismatch. On the expert side, the following theorem bounds the performance difference between the soft-optimal policies of the two different MDPs $M_{\theta^*}^E$ and $M_{\theta^*}^L$ defined in Section 2:

Theorem 1. Consider the two MDPs $M_{\theta^*}^E$ and $M_{\theta^*}^L$ (cf., Section 2) that differ only in the transition dynamics. Let $\pi_{M_{\theta^*}^E}^{\text{soft}}$ and $\pi_{M_{\theta^*}^L}^{\text{soft}}$ be the soft optimal policies for $M_{\theta^*}^E$ and $M_{\theta^*}^L$ respectively. Assume that the true reward function is bounded, i.e., $R_{\theta^*}(s) \in [R_{\min}, R_{\max}]$, $\forall s \in \mathcal{S}$. Then, the state occupancy measures induced by the policies $\pi_{M_{\theta^*}^E}^{\text{soft}}$ and $\pi_{M_{\theta^*}^L}^{\text{soft}}$ on the MDP M^E satisfy the following:

$$\left\| \rho_{M^E}^{\pi_{M_{\theta^*}^E}^{\text{soft}}} - \rho_{M^E}^{\pi_{M_{\theta^*}^L}^{\text{soft}}} \right\|_1 \leq \frac{4 \cdot C}{(1 - \gamma)^2} \cdot \max_{s,a} \sqrt{\|T^E(\cdot | s, a) - T^L(\cdot | s, a)\|_1},$$

where $C = \sqrt{\gamma \cdot \max\{R_{\max} + \log|\mathcal{A}|, -\log|\mathcal{A}| - R_{\min}\}}$. Further, the performance gap between the two policies $\pi_{M_{\theta^*}^E}^{\text{soft}}$ and $\pi_{M_{\theta^*}^L}^{\text{soft}}$ on the MDP $M_{\theta^*}^E$ is bounded as follows:

$$\left| V_{M_{\theta^*}^E}^{\pi_{M_{\theta^*}^E}^{\text{soft}}} - V_{M_{\theta^*}^L}^{\pi_{M_{\theta^*}^L}^{\text{soft}}} \right| \leq \frac{4 \cdot C \cdot R_{\max}^{\text{abs}}}{(1-\gamma)^3} \cdot \max_{s,a} \sqrt{\|T^E(\cdot | s, a) - T^L(\cdot | s, a)\|_1},$$

where $R_{\max}^{\text{abs}} = \max\{|R_{\min}|, |R_{\max}|\}$.

We now turn to our objective. Consider the learner (soft-max) policies obtained as the solutions to the optimization problem (1)-(2):

1. $\pi_{M_{\theta^E}^L}^{\text{soft}}$, when there is a transition dynamics mismatch between the learner and expert,
2. $\pi_{M_{\theta^L}^L}^{\text{soft}}$, when both the learner and expert environments are the same.

The following theorem bounds the performance degradation of policy $\pi_{M_{\theta^E}^L}^{\text{soft}}$ as compared to the policy $\pi_{M_{\theta^L}^L}^{\text{soft}}$ in the MDP $M_{\theta^*}^L$, where the learner operates on:

Theorem 2. *The performance gap between policies $\pi_{M_{\theta^E}^L}^{\text{soft}}$ and $\pi_{M_{\theta^L}^L}^{\text{soft}}$ on the MDP $M_{\theta^*}^L$ is given by*

$$\begin{aligned} \left| V_{M_{\theta^*}^L}^{\pi_{M_{\theta^L}^L}^{\text{soft}}} - V_{M_{\theta^*}^L}^{\pi_{M_{\theta^E}^L}^{\text{soft}}} \right| &\leq \frac{4 \cdot C \cdot R_{\max}^{\text{abs}}}{(1-\gamma)^3} \cdot \max_{s,a} \sqrt{\|T^L(\cdot | s, a) - T^E(\cdot | s, a)\|_1} \\ &\quad + \frac{\gamma \cdot R_{\max}^{\text{abs}}}{(1-\gamma)^2} \cdot \max_{s,a} \|T^L(\cdot | s, a) - T^E(\cdot | s, a)\|_1, \end{aligned}$$

where C and R_{\max}^{abs} are defined as in Theorem 1.

Proofs of Theorems 1 and 2 are in Appendix C.

3.1 Existence of Solution under Transition Dynamics Mismatch

The proof of the existence of a unique solution to the optimization problem (1)-(2), presented in [31], relies on the fact that both expert and learner environments are the same. This assumption implies that the expert policy is in the feasible set that is consequently non-empty. The following theorem poses a condition under which we can ensure that the feasible set is not empty when expert and learner environments are not the same.

Theorem 3. *Consider the matrix \mathbf{T} defined as follows. In the first $|\mathcal{S}|$ rows, the entry in the s^{th} row and $(s'|\mathcal{A}| + a')^{\text{th}}$ column is the element $\rho(s')T^L(s|s', a')$. In the last $|\mathcal{S}|$ rows, the entries are instead given by 1 from position $s'|\mathcal{A}|$ to position $s'|\mathcal{A}| + |\mathcal{A}|$. Then, the feasible set of the optimization problem (1)-(2) is not empty when \mathbf{T} is full rank.*

Proof of Theorem 3 is in Appendix C.4.2. This result allows us to develop a robust MCE IRL scheme in the next section by ensuring the absence of duality gap.

4 Robust MCE IRL via Two-Player Markov Game

This section focuses on recovering a learner (soft-max) policy via MCE IRL framework in a robust manner, under transition dynamics mismatch, i.e., $\rho = \rho_{M_{\theta^*}^E}^{\pi_{M_{\theta^*}^E}^{\text{soft}}}$ in Eq. (2). In particular, our learner policy matches the expert state occupancy measure ρ under the most adversarial transition dynamics belonging to a set described as follows for a given $\alpha > 0$:

$$\mathcal{T}^{L,\alpha} = \{ \alpha T^L + (1-\alpha)\bar{T}, \quad \forall \bar{T} \in \Delta_{\mathcal{S}|\mathcal{S},\mathcal{A}} \}, \quad (3)$$

where $\Delta_{\mathcal{S}|\mathcal{S},\mathcal{A}}$ is the set of all the possible transition dynamics $T : \mathcal{S} \times \mathcal{S} \times \mathcal{A} \rightarrow [0, 1]$.

Note that the transition dynamics in the set $\mathcal{T}^{L,\alpha}$ are perturbed variants of T^L . Then, we define a corresponding class of MDPs as follows:

$$\mathcal{M}^{L,\alpha} = \left\{ \left\{ \mathcal{S}, \mathcal{A}, T^{L,\alpha}, \gamma, P_0 \right\}, \quad \forall T^{L,\alpha} \in \mathcal{T}^{L,\alpha} \right\}.$$

In the following, we systematically derive a robust variant of MCE IRL given in Algorithm 1².

We start by formulating the IRL problem for any MDP $M^{L,\alpha} \in \mathcal{M}^{L,\alpha}$, with transition dynamics $T^{L,\alpha} = \alpha T^L + (1 - \alpha)\bar{T} \in \mathcal{T}^{L,\alpha}$, as follows:

$$\arg \max_{\pi^{\text{pl}} \in \Pi} \mathbb{E} \left[\sum_{t=0}^{\infty} -\gamma^t \log \pi^{\text{pl}}(a_t | s_t) \mid \pi^{\text{pl}}, M^{L,\alpha} \right] \quad (4)$$

$$\text{subject to } \boldsymbol{\rho} = \boldsymbol{\rho}_{M^{L,\alpha}}^{\pi^{\text{pl}}} \quad (5)$$

If Theorem 3 holds, the feasible set is not empty, and the problem can be relaxed without duality gap:

$$\arg \max_{\pi^{\text{pl}} \in \Pi} \mathbb{E} \left[\sum_{t=0}^{\infty} -\gamma^t \log \pi^{\text{pl}}(a_t | s_t) \mid \pi^{\text{pl}}, M^{L,\alpha} \right] + \boldsymbol{\theta}^\top \left(\boldsymbol{\rho}_{M^{L,\alpha}}^{\pi^{\text{pl}}} - \boldsymbol{\rho} \right) \quad (6)$$

For any fixed $\boldsymbol{\theta} \in \mathbb{R}^{|\mathcal{S}|}$ the problem (6) is feasible since Π is a closed and bounded set.

We define $U(\boldsymbol{\theta})$ as the value of the program (6) for a given $\boldsymbol{\theta}$. By weak duality, $U(\boldsymbol{\theta})$ provides an upper bound on the optimization problem (4)-(5). Consequently, we introduce the dual problem aiming to find the value of $\boldsymbol{\theta}$ corresponding to the lowest upper bound, which can be written as

$$\min_{\boldsymbol{\theta}} U(\boldsymbol{\theta}) := \max_{\pi^{\text{pl}} \in \Pi} \mathbb{E} \left[\sum_{t=0}^{\infty} -\gamma^t \log \pi^{\text{pl}}(a_t | s_t) \mid \pi^{\text{pl}}, M^{L,\alpha} \right] + \boldsymbol{\theta}^\top \left(\boldsymbol{\rho}_{M^{L,\alpha}}^{\pi^{\text{pl}}} - \boldsymbol{\rho} \right). \quad (7)$$

We then define $\pi^{\text{pl},*}$ as follows

$$\pi^{\text{pl},*} \in \arg \max_{\pi^{\text{pl}} \in \Pi} \boldsymbol{\theta}^\top \boldsymbol{\rho}_{M^{L,\alpha}}^{\pi^{\text{pl}}} + \mathbb{E} \left[\sum_{t=0}^{\infty} -\gamma^t \log \pi^{\text{pl}}(a_t | s_t) \mid \pi^{\text{pl}}, M^{L,\alpha} \right].$$

One can compute the gradient³ $\nabla_{\boldsymbol{\theta}} U = \boldsymbol{\rho}_{M^{L,\alpha}}^{\pi^{\text{pl},*}} - \boldsymbol{\rho}$, and thus update the parameter simply as $\boldsymbol{\theta} \leftarrow \boldsymbol{\theta} - \nabla U$ or with a more sophisticated optimization scheme. According to [32, Theorem 1], the policy $\pi^{\text{pl},*}$ exists and it is unique. If Theorem 3 holds, then the problem can be relaxed without duality gap according to [31, Lemma 2].

Based on these observations, we propose to maximize the primal objective in the MDP $M^{L,\alpha,\boldsymbol{\theta}} \in \mathcal{M}^{L,\alpha}$ that minimizes the entropy regularized total expected return of the player with respect to the parameter $\boldsymbol{\theta}$, i.e., $M^{L,\alpha,\boldsymbol{\theta}} \in \arg \min_{M \in \mathcal{M}^{L,\alpha}} \boldsymbol{\theta}^\top \boldsymbol{\rho}_M^{\pi^{\text{pl}}} + \mathbb{E} \left[\sum_{t=0}^{\infty} -\gamma^t \log \pi^{\text{pl}}(a_t | s_t) \mid \pi^{\text{pl}}, M \right]$.⁴

To this end, we need to solve the following problem:

$$\arg \max_{\pi^{\text{pl}} \in \Pi} \min_{M \in \mathcal{M}^{L,\alpha}} \mathbb{E} \left[\sum_{t=0}^{\infty} -\gamma^t \log \pi^{\text{pl}}(a_t | s_t) \mid \pi^{\text{pl}}, M \right] + \boldsymbol{\theta}^\top \boldsymbol{\rho}_M^{\pi^{\text{pl}}}, \quad (8)$$

where the term depending $\boldsymbol{\rho}$ has been neglected since it is not affected by the variables of the optimization problem. We can express the entropy term in the above problem as follows:

$$\begin{aligned} \mathbb{E} \left[\sum_{t=0}^{\infty} -\gamma^t \log \pi^{\text{pl}}(a_t | s_t) \mid \pi^{\text{pl}}, M \right] &= \sum_{s \in \mathcal{S}} \rho_M^{\pi^{\text{pl}}}(s) \sum_{a \in \mathcal{A}} \{ -\pi^{\text{pl}}(a | s) \log \pi^{\text{pl}}(a | s) \} \\ &= \sum_{s \in \mathcal{S}} \rho_M^{\pi^{\text{pl}}}(s) H^{\pi^{\text{pl}}}(A | S = s) \end{aligned}$$

²The gradient $\boldsymbol{\rho}_{M^{L,\alpha}}^{\alpha\pi^{\text{pl}}+(1-\alpha)\pi^{\text{op}}} - \boldsymbol{\rho}$ is equivalent to $\boldsymbol{\rho}_{M^{L,\alpha,\boldsymbol{\theta}}}^{\pi^{\text{pl}}} - \boldsymbol{\rho}$.

³We have verified in Appendix D that the same update arises as gradient of the worst-case predictive log-loss modified to take into account the transition dynamics mismatch.

⁴Note that as the parameter $\boldsymbol{\theta}$ is updated, the worst case environment also changes. As long as the environment $M^{L,\alpha,\boldsymbol{\theta}}$ satisfies the requirement of Theorem 3, our procedure holds.

$$= \left(\mathbf{H}^{\pi^{\text{pl}}} \right)^\top \boldsymbol{\rho}_M^{\pi^{\text{pl}}},$$

where $\mathbf{H}^{\pi^{\text{pl}}} \in \mathbb{R}^{|S|}$ a vector whose s^{th} element is the entropy of the player policy given the state s . Since the quantity $\mathbf{H}^{\pi^{\text{pl}}} + \boldsymbol{\theta}$ depends only on the states, to solve the problem (8), we can utilize the equivalence between the *robust MDP* [27, 28] formulation and the *action-robust MDP* [29, 26, 33] formulation shown in [26]. We can interpret the minimization over the environment class as the minimization over a set of opponent policies that with probability $1 - \alpha$ take control of the agent and perform the worst possible move from the current agent state. Indeed, interpreting $\left(\mathbf{H}^{\pi^{\text{pl}}} + \boldsymbol{\theta} \right)^\top \boldsymbol{\rho}_M^{\pi^{\text{pl}}}$ as an entropy regularized value function, i.e., $\boldsymbol{\theta}$ as a reward parameter, we can write:

$$\begin{aligned} & \min_{M \in \mathcal{M}^{L,\alpha}} \left(\mathbf{H}^{\pi^{\text{pl}}} + \boldsymbol{\theta} \right)^\top \boldsymbol{\rho}_M^{\pi^{\text{pl}}} \\ &= \min_T \mathbb{E} \left[\sum_{t=0}^{\infty} \gamma^t \left\{ R_{\boldsymbol{\theta}}(s_t) + H^{\pi^{\text{pl}}}(A | S = s_t) \right\} \middle| \pi^{\text{pl}}, P_0, \alpha T^L + (1 - \alpha)\bar{T} \right] \\ &= \min_{\pi^{\text{op}} \in \Pi} \mathbb{E} \left[\sum_{t=0}^{\infty} \gamma^t \left\{ R_{\boldsymbol{\theta}}(s_t) + H^{\pi^{\text{pl}}}(A | S = s_t) \right\} \middle| \alpha \pi^{\text{pl}} + (1 - \alpha)\pi^{\text{op}}, M^L \right]. \quad (9) \end{aligned}$$

Finally, we can formulate the problem (9) as a two-player zero-sum Markov game [26] with transition dynamics given by

$$T^{\text{two},L,\alpha}(s' | s, a^{\text{pl}}, a^{\text{op}}) = \alpha T^L(s' | s, a^{\text{pl}}) + (1 - \alpha)T^L(s' | s, a^{\text{op}}),$$

where a^{pl} is an action chosen according to the player policy and a^{op} according to the opponent policy.

Note that the opponent is restricted to take the worst possible action from the state of the player, i.e., there is no additional state variable for the opponent. As a result, we reach a two-player Markov game with a regularization term for the player as follows:

$$\arg \max_{\pi^{\text{pl}} \in \Pi} \min_{\pi^{\text{op}} \in \Pi} \mathbb{E} \left[\sum_{t=0}^{\infty} \gamma^t \left\{ R_{\boldsymbol{\theta}}(s_t) + H^{\pi^{\text{pl}}}(A | S = s_t) \right\} \middle| \pi^{\text{pl}}, \pi^{\text{op}}, M^{\text{two},L,\alpha} \right], \quad (10)$$

where $M^{\text{two},L,\alpha} = \{S, \mathcal{A}, \mathcal{A}, T^{\text{two},L,\alpha}, \gamma, P_0, R_{\boldsymbol{\theta}}\}$ is the two-player MDP associated with the above game. The repetition of the action space \mathcal{A} denotes the fact that player and adversary share the same action space. We propose a dynamic programming approach to find player and opponent policies (*cf.*, Algorithm 2). Theoretical support (inspired from [34]) for the Algorithm 2 is provided in Appendix E.

Algorithm 1 Robust MCE IRL via Markov Game

Initialize: Player policy π^{pl} , opponent strength α , opponent policy π^{op} , parameter $\boldsymbol{\theta}$
while not converged **do**
 Compute $\boldsymbol{\rho}_{M^L}^{\alpha\pi^{\text{pl}}+(1-\alpha)\pi^{\text{op}}}$ by dynamic programming (*cf.*, [31, Section V.C]).
 Update $\boldsymbol{\theta}$ with Adam [35] using the gradient $\left(\boldsymbol{\rho}_{M^L}^{\alpha\pi^{\text{pl}}+(1-\alpha)\pi^{\text{op}}} - \boldsymbol{\rho} \right)$.
 Use Algorithm 2 with $R = R_{\boldsymbol{\theta}}$ to update π^{pl} and π^{op} s.t. they solve the problem (10).
end while

5 Experiments

This section demonstrates the superior performance due our robust method as compared to the standard MCE IRL algorithm, when there is a transition dynamics mismatch between the expert and the learner. We also assess the effect of the parameter choices α .

Setup: We consider a reference MDP $M_{\boldsymbol{\theta}^*}^{\text{ref}} = (S, \mathcal{A}, T^{\text{ref}}, \gamma, P_0, R_{\boldsymbol{\theta}^*})$ with deterministic transition dynamics T^{ref} . Further, given a *learner noise* $\epsilon_L \in [0, 1]$, we introduce a learner MDP without reward function as $M^{L,\epsilon_L} = (S, \mathcal{A}, T^{L,\epsilon_L}, \gamma, P_0)$ where $T^{L,\epsilon_L} \in \Delta_{S|S,\mathcal{A}}$ is defined as $T^{L,\epsilon_L} := (1 - \epsilon_L)T^{\text{ref}} + \epsilon_L\bar{T}$ with $\bar{T} \in \Delta_{S|S,\mathcal{A}}$.

Algorithm 2 Value Iteration for Two-Player Markov Game

Initialize: $Q(s, a^{\text{pl}}, a^{\text{op}}) \leftarrow 0, V(s) \leftarrow 0$ **while** not converged **do** **for** $s \in \mathcal{S}$ **do** **for** $(a^{\text{pl}}, a^{\text{op}}) \in \mathcal{A} \times \mathcal{A}$ **do**

$$Q(s, a^{\text{pl}}, a^{\text{op}}) = R(s) + \gamma \sum_{s'} T^{\text{two}, L, \alpha}(s'|s, a^{\text{pl}}, a^{\text{op}}) V(s') \quad (11)$$

end for

$$V(s) = \log \sum_{a^{\text{pl}}} \exp \left(\min_{a^{\text{op}}} Q(s, a^{\text{pl}}, a^{\text{op}}) \right) \quad (12)$$

end for**end while**Compute the marginal Q values for player and opponent, for all $(s, a^{\text{pl}}, a^{\text{op}}) \in \mathcal{S} \times \mathcal{A} \times \mathcal{A}$:

$$Q^{\text{pl}}(s, a^{\text{pl}}) = \min_{a^{\text{op}}} Q(s, a^{\text{pl}}, a^{\text{op}}) \quad \text{and} \quad Q^{\text{op}}(s, a^{\text{op}}) = \log \sum_{a^{\text{pl}}} \exp Q(s, a^{\text{pl}}, a^{\text{op}}) \quad (13)$$

Compute the player (soft-max) and opponent (greedy) policies, for all $(s, a^{\text{pl}}, a^{\text{op}}) \in \mathcal{S} \times \mathcal{A} \times \mathcal{A}$:

$$\pi^{\text{pl}}(a^{\text{pl}}|s) = \frac{\exp Q^{\text{pl}}(s, a^{\text{pl}})}{\sum_{a'} \exp Q^{\text{pl}}(s, a')} \quad \text{and} \quad \pi^{\text{op}}(a^{\text{op}}|s) = \mathbb{1} \left[a^{\text{op}} \in \arg \min_{a'} Q^{\text{op}}(s, a') \right]$$

Output: π^{pl} and π^{op}

Similarly, given an *expert noise* $\epsilon_E \in [0, 1]$, we define an expert MDP $M_{\theta^*}^{E, \epsilon_E} = (\mathcal{S}, \mathcal{A}, T^{E, \epsilon_E}, \gamma, P_0, R_{\theta^*})$ where $T^{E, \epsilon_E} \in \Delta_{\mathcal{S}|\mathcal{S}, \mathcal{A}}$ is defined as $T^{E, \epsilon_E} := (1 - \epsilon_E)T^{\text{ref}} + \epsilon_E \bar{T}$ with $\bar{T} \in \Delta_{\mathcal{S}|\mathcal{S}, \mathcal{A}}$. Notice that fixing a pair (ϵ_E, ϵ_L) defines a precise IRL problem with model mismatch where the expert acts in $M_{\theta^*}^{E, \epsilon_E}$ and the learner in M^{L, ϵ_L} . For each fixed noise pairs (ϵ_E, ϵ_L) , we apply our approach with different values for α , whereby obtaining a different policy for each tuple $(\epsilon_E, \epsilon_L, \alpha)$. We finally evaluate the total expected return of each of these recovered policies in $M_{\theta^*}^{L, \epsilon_L}$, i.e., M^{L, ϵ_L} endowed with the true reward function R_{θ^*} for each value of α .

Environments: We study the classical environments **Gridworld** and **Objectworld**, whose reward functions are linear and non-linear, respectively. Both of them are $N \times N$ grid, where a cell represents a state, with four actions per state, corresponding to steps in one of the four cardinal directions.

Gridworld has a linear reward represented by a weight vector with entries corresponding to each state, as shown in Figure 2a. Introduced by [36], Objectworld is a gridworld with non-linear reward determined by the distance of the agent to the objects that are randomly placed in the environment.

Each object has an outer and an inner color; however, only the former plays a role in determining the reward while the latter serves as a distractor. The reward is -2 in positions within three cells to an outer blue object (black areas of Figure 2e), 0 if they are also within two cells from an outer green object (white areas), and -1 otherwise (gray areas).

To accommodate the infinite horizon setting in MCE IRL, we shift the rewards originally proposed by [36] to non-positive values, and we randomly placed the goal state in a white area. We also modify the reward features originally proposed in [36] by augmenting them with binary features indicating whether the goal state has been reached. In order to face reward non-linearity, we applied our scheme using a neural network as reward approximator [37]. The network architecture is in Appendix F.

Results: The numerical results can be found in Figure 2, where we consider a Gridworld environment with a negative area in the middle and safe path along the side of the domain. In Figure 2b we present the results when $\epsilon_L = 0$. Our expected improvements are confirmed by this toy problem.

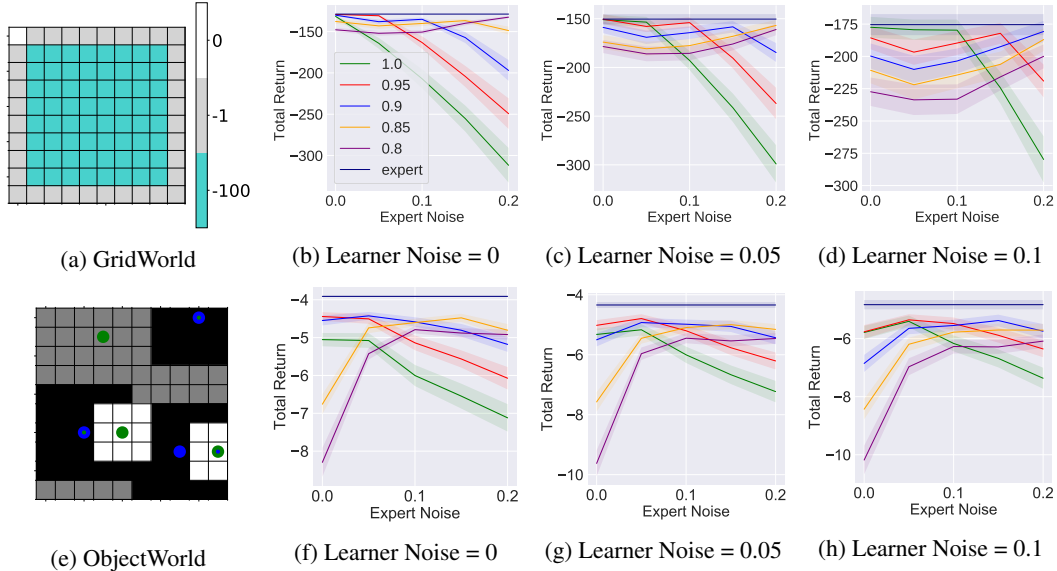


Figure 2: On the x-axis, we report different expert noises ϵ_E , while the y-axis indicates the total expected return for the policy that is recovered from the expert acting in $M_{\theta^*}^{E, \epsilon_E}$, varying α . All the recovered policies are evaluated on the learner MDP endowed with the true reward $M_{\theta^*}^{L, \epsilon_L}$. The expert baseline in the plots is the policy obtained in $M_{\theta^*}^{L, \epsilon_L}$ applying Value-Iteration. Since it is a baseline independent from the IRL procedure, it is constant for all the different ϵ_E . It represents the best performance that can be achieved by a policy in $M_{\theta^*}^{L, \epsilon_L}$. The fact that our algorithm produces similar performance to this reference means that our method not only improves over MCE IRL but also that it can be nearly optimal provided that α is properly tuned. We decided to adopt a uniform \bar{T} in defining $M_{\theta^*}^{E, \epsilon_E}$ and $M_{\theta^*}^{L, \epsilon_L}$, and we tested all the possible pairs picking ϵ_L from the set $\{0.0, 0.05, 0.1\}$ and ϵ_E from $\{0.0, 0.05, 0.1, 0.15, 0.2\}$. Each plot reports the results for a fixed ϵ_L . The values used for α are reported in the legend.

Indeed, the MCE IRL performance⁵ is seen to almost match the expert policy without mismatch, but it becomes quickly less preferable as the expert noise ϵ_E increases. On the other extreme, our method with $\alpha = 0.8$ is too conservative when $\epsilon_E = 0$, but it recovers the best performing policy when the $\epsilon_E = 0.2$. The same experiment is repeated for $\epsilon_L = 0.05$ in Figure 2c and for $\epsilon_L = 0.1$ in Figure 2d. Similar behavior is observed, but the MCE IRL performance decay starts at a much higher noise.

A similar trend is observed in Objectworld, as shown in Figures 2f, 2g, and 2h, and on other Gridworlds reported in Appendix F. Consequently, the empirical experiments confirm that our algorithm improves over the standard MCE IRL in case of model mismatch if α is such that T^{E, ϵ_E} falls in the class $\mathcal{T}^{L, \alpha}$. Overestimating the class’s necessary size worsens the performance.

6 Related Work

Generative Adversarial Imitation Learning (GAIL) [38] and its variants are IRL methods that use a GAN-based reward to align the distribution of the state-action pairs between the expert and the learner. When there is a transition dynamics mismatch, the expert’s actions are not quite useful for imitation. [39, 40] have considered state only distribution matching when the expert actions are not observable. Building on these works, [21, 22] have studied the imitation learning problem under transition dynamics mismatch. These works propose some sophisticated model-alignment based imitation learning algorithms in the high dimensional settings to address the dynamics mismatch.

⁵MCE IRL is indicated by the line labeled as $\alpha = 1$ in Figure 2. Notice, indeed, that our method with $\alpha = 1$ recovers the standard MCE IRL.

7 Conclusions

In this work, we theoretically analyze the transition dynamics mismatch issue in IRL in the finite MDP setting. We also propose a robust MCE IRL algorithm, and empirically demonstrate its efficacy. As future work, we plan to extend our analysis and action-robustness approach to high dimensional continuous control setting with appropriate practical relaxations.

Broader Impact

We address the transition dynamics mismatch issue in the inverse reinforcement with a theoretically grounded algorithm and demonstrate its efficacy via extensive experiments. Our results apply to the finite MDP setting. Once we extend our work to the high dimensional and continuous control setting, it would be widely useful to the control/RL community. Nevertheless, we want to highlight the importance of robustness in IRL, especially when it comes to topics related to safety, such as autonomous driving and healthcare. Even though our adversarial training method improves robustness, being overly conservative might result in lower performance. Thus one should carefully tune the robustness related hyperparameters, which is α in our case.

Acknowledgments and Disclosure of Funding

This work has received funding from the European Research Council (ERC) under the European Union’s Horizon 2020 research and innovation program (grant agreement n 725594 - time-data), and the Swiss National Science Foundation (SNSF) under grant number 407540_167319.

References

- [1] Richard S Sutton, David A McAllester, Satinder P Singh, and Yishay Mansour. Policy gradient methods for reinforcement learning with function approximation. In *Advances in neural information processing systems*, pages 1057–1063, 2000.
- [2] David Silver, Guy Lever, Nicolas Heess, Thomas Degris, Daan Wierstra, and Martin Riedmiller. Deterministic policy gradient algorithms. In *Proceedings of the 31st International Conference on International Conference on Machine Learning-Volume 32*, pages I–387, 2014.
- [3] John Schulman, Sergey Levine, Pieter Abbeel, Michael Jordan, and Philipp Moritz. Trust region policy optimization. In *International conference on machine learning*, pages 1889–1897, 2015.
- [4] John Schulman, Filip Wolski, Prafulla Dhariwal, Alec Radford, and Oleg Klimov. Proximal policy optimization algorithms. *arXiv preprint arXiv:1707.06347*, 2017.
- [5] Volodymyr Mnih, Koray Kavukcuoglu, David Silver, Andrei A Rusu, Joel Veness, Marc G Bellemare, Alex Graves, Martin Riedmiller, Andreas K Fidjeland, Georg Ostrovski, et al. Human-level control through deep reinforcement learning. *Nature*, 518(7540):529–533, 2015.
- [6] David Silver, Julian Schrittwieser, Karen Simonyan, Ioannis Antonoglou, Aja Huang, Arthur Guez, Thomas Hubert, Lucas Baker, Matthew Lai, Adrian Bolton, et al. Mastering the game of go without human knowledge. *Nature*, 550(7676):354–359, 2017.
- [7] Timothy P Lillicrap, Jonathan J Hunt, Alexander Pritzel, Nicolas Heess, Tom Erez, Yuval Tassa, David Silver, and Daan Wierstra. Continuous control with deep reinforcement learning. *arXiv preprint arXiv:1509.02971*, 2015.
- [8] Sergey Levine, Chelsea Finn, Trevor Darrell, and Pieter Abbeel. End-to-end training of deep visuomotor policies. *The Journal of Machine Learning Research*, 17(1):1334–1373, 2016.
- [9] Stuart Russell. Learning agents for uncertain environments. In *Conference on Learning Theory*, pages 101–103, 1998.
- [10] Andrew Y Ng and Stuart Russell. Algorithms for inverse reinforcement learning. In *Proc. Intl Conf. on Machine Learning (ICML)*, 2000.

- [11] Pieter Abbeel and Andrew Y Ng. Apprenticeship learning via inverse reinforcement learning. In *Proc. Intl Conf. on Machine Learning (ICML)*, 2004.
- [12] Nathan D Ratliff, J Andrew Bagnell, and Martin A Zinkevich. Maximum margin planning. In *ICML*, pages 729–736, 2006.
- [13] Brian D Ziebart, Andrew L Maas, J Andrew Bagnell, and Anind K Dey. Maximum entropy inverse reinforcement learning. In *Proc. AAAI Conference on Artificial Intelligence*, 2008.
- [14] Umar Syed and Robert E Schapire. A game-theoretic approach to apprenticeship learning. In *Advances in neural information processing systems*, pages 1449–1456, 2008.
- [15] Abdeslam Boularias, Jens Kober, and Jan Peters. Relative entropy inverse reinforcement learning. In *AISTATS*, pages 182–189, 2011.
- [16] T Osa, J Pajarinen, G Neumann, JA Bagnell, P Abbeel, and J Peters. An algorithmic perspective on imitation learning. *Foundations and Trends in Robotics*, 7(1-2):1–179, 2018.
- [17] Chao Yu, Jiming Liu, and Shamim Nemati. Reinforcement learning in healthcare: A survey, 2019.
- [18] B Ravi Kiran, Ibrahim Sobh, Victor Talpaert, Patrick Mannion, Ahmad A Al Sallab, Senthil Yogamani, and Patrick Pérez. Deep reinforcement learning for autonomous driving: A survey. *arXiv preprint arXiv:2002.00444*, 2020.
- [19] Sid Reddy, Anca Dragan, and Sergey Levine. Where do you think you’re going?: Inferring beliefs about dynamics from behavior. In *Advances in Neural Information Processing Systems*, pages 1454–1465, 2018.
- [20] Ze Gong and Yu Zhang. What is it you really want of me? generalized reward learning with biased beliefs about domain dynamics. In *AAAI 2020*, 2020.
- [21] Tanmay Gangwani and Jian Peng. State-only imitation with transition dynamics mismatch, 2020.
- [22] Fangchen Liu, Zhan Ling, Tongzhou Mu, and Hao Su. State alignment-based imitation learning, 2019.
- [23] Brian D Ziebart. *Modeling purposeful adaptive behavior with the principle of maximum causal entropy*. PhD thesis, Carnegie Mellon University, 2010.
- [24] Brian D Ziebart, J Andrew Bagnell, and Anind K Dey. The principle of maximum causal entropy for estimating interacting processes. *IEEE Transactions on Information Theory*, 59(4):1966–1980, 2013.
- [25] Zhengyuan Zhou, Michael Bloem, and Nicholas Bambos. Infinite time horizon maximum causal entropy inverse reinforcement learning. *IEEE Transactions on Automatic Control*, 63(9):2787–2802, 2017.
- [26] Chen Tessler, Yonathan Efroni, and Shie Mannor. Action robust reinforcement learning and applications in continuous control, 2019.
- [27] Garud N Iyengar. Robust dynamic programming. *Mathematics of Operations Research*, 30(2):257–280, 2005.
- [28] Arnab Nilim and Laurent El Ghaoui. Robust control of markov decision processes with uncertain transition matrices. *Operations Research*, 53(5):780–798, 2005.
- [29] Lerrel Pinto, James Davidson, Rahul Sukthankar, and Abhinav Gupta. Robust adversarial reinforcement learning. In *International Conference on Machine Learning*, pages 2817–2826, 2017.
- [30] Serge Herman, Tobias Gindele, Jörg Wagner, Felix Schmitt, and Wolfram Burgard. Inverse reinforcement learning with simultaneous estimation of rewards and dynamics. *ArXiv*, abs/1604.03912, 2016.

- [31] M. Bloem and N. Bambos. Infinite time horizon maximum causal entropy inverse reinforcement learning. In *53rd IEEE Conference on Decision and Control*, pages 4911–4916, 2014.
- [32] Matthieu Geist, Bruno Scherrer, and Olivier Pietquin. A theory of regularized markov decision processes. *CoRR*, abs/1901.11275, 2019.
- [33] Parameswaran Kamalaruban, Yu-Ting Huang, Ya-Ping Hsieh, Paul Rolland, Cheng Shi, and Volkan Cevher. Robust reinforcement learning via adversarial training with langevin dynamics. *arXiv preprint arXiv:2002.06063*, 2020.
- [34] Jordi Grau-Moya, Felix Leibfried, and Haitham Bou-Ammar. Balancing two-player stochastic games with soft q-learning. *arXiv preprint arXiv:1802.03216*, 2018.
- [35] Diederik P. Kingma and Jimmy Ba. Adam: A method for stochastic optimization, 2014.
- [36] Sergey Levine, Zoran Popovic, and Vladlen Koltun. Nonlinear inverse reinforcement learning with gaussian processes. In J. Shawe-Taylor, R. S. Zemel, P. L. Bartlett, F. Pereira, and K. Q. Weinberger, editors, *Advances in Neural Information Processing Systems 24*, pages 19–27. Curran Associates, Inc., 2011.
- [37] Markus Wulfmeier, Peter Ondruska, and Ingmar Posner. Maximum entropy deep inverse reinforcement learning. *arXiv:1507.04888*, 2015.
- [38] Jonathan Ho and Stefano Ermon. Generative adversarial imitation learning. In *Advances in Neural Information Processing Systems (NeurIPS)*, 2016.
- [39] Faraz Torabi, Garrett Warnell, and Peter Stone. Generative adversarial imitation from observation, 2018.
- [40] Wen Sun, Anirudh Vemula, Byron Boots, and J. Andrew Bagnell. Provably efficient imitation learning from observation alone, 2019.
- [41] Wen Sun, Geoffrey J Gordon, Byron Boots, and J. Bagnell. Dual policy iteration. In S. Bengio, H. Wallach, H. Larochelle, K. Grauman, N. Cesa-Bianchi, and R. Garnett, editors, *Advances in Neural Information Processing Systems 31*, pages 7059–7069. Curran Associates, Inc., 2018.
- [42] Michael J. Kearns and Satinder P. Singh. Near-optimal reinforcement learning in polynomial time. In *Proceedings of the Fifteenth International Conference on Machine Learning, ICML '98*, page 260–268, San Francisco, CA, USA, 1998. Morgan Kaufmann Publishers Inc.
- [43] Abdeslam Boularias and Brahim Chaib-draa. Bootstrapping apprenticeship learning. In J. D. Lafferty, C. K. I. Williams, J. Shawe-Taylor, R. S. Zemel, and A. Culotta, editors, *Advances in Neural Information Processing Systems 23*, pages 289–297. Curran Associates, Inc., 2010.
- [44] Kamalaruban Parameswaran, Rati Devidze, Volkan Cevher, and Adish Singla. Interactive teaching algorithms for inverse reinforcement learning. In *The 28th International Joint Conference on Artificial Intelligence*, 2019.

A Appendix structure

This Appendix provides additional proofs and experimental results. Here we provide an overview on the organization of the section.

- Appendix B reports omitted facts of Section 2,
- Appendix C reports the proofs of Theorems 1, 2 and 3. In addition it presents the statement and proof of Theorem 4 that is needed as intermediate step to prove Theorem 2.
- Appendix D gives additional insight on the gradient computation under model mismatch recasting the causal entropy maximization as a worst case predictive log-loss minimization problem.
- Appendix E provides support to Algorithm 2.
- Appendix F contains additional experimental results and details on their execution.

B Further Details of Section 2

Bellman Optimality Equations. An optimal policy $\pi_{M_\theta}^*$ is optimal for the MDP M_θ if $\pi \in \arg \max_{\pi'} V_{M_\theta}^{\pi'}$. This is equivalent to require that $\pi_{M_\theta}^*$ satisfies the following recursion known as *Bellman optimality equations* for all state action pairs $(s, a) \in \mathcal{S} \times \mathcal{A}$:

$$\begin{aligned}\pi_{M_\theta}^*(s) &= \arg \max_a Q_{M_\theta}^*(s, a) \\ Q_{M_\theta}^*(s, a) &= R_\theta(s, a) + \gamma \sum_{s'} T(s'|s, a) V_{M_\theta}^*(s') \\ V_{M_\theta}^*(s) &= \max_a Q_{M_\theta}^*(s, a)\end{aligned}$$

Soft Bellman Optimality Equations. The *soft-optimal* policy (always unique) in M_θ is defined as $\pi_{M_\theta}^{\text{soft}} := \arg \max_{\pi'} V_{M_\theta}^{\pi', \text{soft}}$. This is equivalent to require that $\pi_{M_\theta}^{\text{soft}}$ satisfies the following recursion known as *soft Bellman optimality equations* for all state action pairs $(s, a) \in \mathcal{S} \times \mathcal{A}$:

$$\begin{aligned}\pi_{M_\theta}^{\text{soft}}(a|s) &= \exp(Q_{M_\theta}^{\text{soft}}(s, a) - V_{M_\theta}^{\text{soft}}(s)) \\ Q_{M_\theta}^{\text{soft}}(s, a) &= R_\theta(s, a) + \gamma \sum_{s'} T(s'|s, a) V_{M_\theta}^{\text{soft}}(s') \\ V_{M_\theta}^{\text{soft}}(s) &= \log \sum_a \exp Q_{M_\theta}^{\text{soft}}(s, a)\end{aligned}$$

Value-Iteration. The Bellman optimality equations suggest that an optimal policy $\pi_{M_\theta}^*$ in M_θ can be computed by finding the optimal value functions $V_{M_\theta}^*$ and $Q_{M_\theta}^*$. In practice, when the transition dynamics are known, they are computed by the algorithm known as *Value-Iteration* that iterates in the following manner until the convergence criterion is not met.

$$\begin{aligned}Q_{M_\theta}^{k+1}(s, a) &= R_\theta(s, a) + \gamma \sum_{s'} T(s'|s, a) V_{M_\theta}^k(s') \\ V_{M_\theta}^k(s) &= \max_a Q_{M_\theta}^k(s, a)\end{aligned}$$

Soft-Value-Iteration. The soft Bellman optimality equations suggest that the soft-optimal policy $\pi_{M_\theta}^{\text{soft}}$ in M_θ can be computed by finding the soft-optimal value functions $V_{M_\theta}^{\text{soft}}$ and $Q_{M_\theta}^{\text{soft}}$. In practice, when the transition dynamics are known, they are computed by the algorithm known as *Soft-Value-Iteration* [31, 23] that iterates in the following manner until the convergence criterion is not met.

$$\begin{aligned}Q_{M_\theta}^{k+1}(s, a) &= R_\theta(s, a) + \gamma \sum_{s'} T(s'|s, a) V_{M_\theta}^k(s') \\ V_{M_\theta}^k(s) &= \log \sum_a \exp Q_{M_\theta}^k(s, a)\end{aligned}$$

B.1 Matching One-hot Features vs. Matching State Occupancy Measures

In most MCE IRL literature, the matching objective is the *expected feature count* $\bar{\phi}_M^\pi$, defined as $\bar{\phi}_M^\pi := \mathbb{E}_{\pi, M} [\sum_{t=0}^{\infty} \gamma^t \phi(s_t)]$, where $\phi(s)$ is a state dependent vector.

Fact 1. *If $\forall s \in \mathcal{S}$, $\phi(s) \in \mathbb{R}^{|\mathcal{S}|}$ is a one-hot vector with only the element in position s being 1, then the expected feature count is proportional to the occupancy measure vector.*

Indeed $\forall M, \pi$, we have:

$$\begin{aligned} \bar{\phi}_M^{\pi_L} &= \mathbb{E}_{\pi, M} \left[\sum_{t=0}^{\infty} \gamma^t \phi(s_t) \right] \\ &= \mathbb{E}_{\pi, M} \left[\sum_{t=0}^{\infty} \gamma^t \sum_{s \in \mathcal{S}} \phi(s) \mathbb{1}[s = s_t] \right] \\ &= \sum_{s \in \mathcal{S}} \phi(s) \mathbb{E}_{\pi, M} \left[\sum_{t=0}^{\infty} \gamma^t \mathbb{1}[s = s_t] \right] \\ &= \sum_{s \in \mathcal{S}} \phi(s) \sum_{t=0}^{\infty} \gamma^t \mathbb{E}_{\pi, M} [\mathbb{1}[s = s_t]] \\ &= \frac{1}{1-\gamma} \sum_{s \in \mathcal{S}} \rho_M^\pi(s) \phi(s) \end{aligned}$$

For the one-hot feature map, ignoring the normalizing factor, the above sum of vectors can be written as follows:

$$[\rho_M^\pi(s'), \rho_M^\pi(s''), \dots]^\top = \boldsymbol{\rho}_M^\pi.$$

Leveraging on this fact, we formulate the MCE IRL problem (1)-(2) with occupancy measure $\boldsymbol{\rho}$ match rather than the usual feature count match. Note that if the occupancy measure match is attained, the match of any expected feature count is also attained.

C Proofs of Section 3

C.1 Proof of Theorem 1

Preliminaries. The soft-optimal policy of M_θ^E satisfies the soft Bellman optimality equations:

$$\pi_{M_\theta^E}^{\text{soft}}(a|s) = \frac{Z_{a|s}^E}{Z_s^E} \quad (14)$$

$$\log Z_s^E = \log \sum_a Z_{a|s}^E$$

$$\log Z_{a|s}^E = R_{\theta^*}(s, a) + \gamma \sum_{s'} T^E(s'|a, s) \log Z_{s'}^E \quad (15)$$

Analogously, soft-optimal policy of M_θ^L :

$$\pi_{M_\theta^L}^{\text{soft}}(a|s) = \frac{Z_{a|s}^L}{Z_s^L} \quad (16)$$

$$\log Z_s^L = \log \sum_a Z_{a|s}^L$$

$$\log Z_{a|s}^L = R_{\theta^*}(s, a) + \gamma \sum_{s'} T^L(s'|a, s) \log Z_{s'}^L \quad (17)$$

Another important point to clarify is that in the proof we overload the symbol ρ_M^π to account also for the state-action occupancy measure, defined as follows:

$$\rho_M^\pi(s, a) := \pi(a|s) \rho_M^\pi(s).$$

Proof. We prove the result for the most general case of state-action dependent reward.

In the following we seek a bound for the total expected return difference, $\left| V_{M_{\theta^*}^E}^{\pi_{M_{\theta^*}^L}^{\text{soft}}} - V_{M_{\theta^*}^E}^{\pi_{M_{\theta^*}^E}^{\text{soft}}} \right|^6$.

$$\begin{aligned}
\left| V_{M_{\theta^*}^E}^{\pi_{M_{\theta^*}^L}^{\text{soft}}} - V_{M_{\theta^*}^E}^{\pi_{M_{\theta^*}^E}^{\text{soft}}} \right| &= \frac{1}{1-\gamma} \left| \sum_{s,a} \left(\rho_{M_{\theta^*}^E}^{\pi_{M_{\theta^*}^L}^{\text{soft}}}(s,a) - \rho_{M_{\theta^*}^E}^{\pi_{M_{\theta^*}^E}^{\text{soft}}}(s,a) \right) R_{\theta^*}(s,a) \right| \\
&\leq \frac{1}{1-\gamma} \sum_{s,a} \left| \rho_{M_{\theta^*}^E}^{\pi_{M_{\theta^*}^L}^{\text{soft}}}(s,a) - \rho_{M_{\theta^*}^E}^{\pi_{M_{\theta^*}^E}^{\text{soft}}}(s,a) \right| |R_{\theta^*}(s,a)| \\
&\leq \frac{R_{\max}^{\text{abs}}}{1-\gamma} \sum_{s,a} \left| \rho_{M_{\theta^*}^E}^{\pi_{M_{\theta^*}^L}^{\text{soft}}}(s,a) - \rho_{M_{\theta^*}^E}^{\pi_{M_{\theta^*}^E}^{\text{soft}}}(s,a) \right| \\
&= \frac{R_{\max}^{\text{abs}}}{1-\gamma} \left\| \rho_{M_{\theta^*}^E}^{\pi_{M_{\theta^*}^L}^{\text{soft}}} - \rho_{M_{\theta^*}^E}^{\pi_{M_{\theta^*}^E}^{\text{soft}}} \right\|_1
\end{aligned} \tag{18}$$

Then, for two policies acting in the same MDP (M^E in our case), it holds that (*cf.*, [41, Lemma A.1]):

$$\left\| \rho_{M^E}^{\pi_{M^L}^{\text{soft}}} - \rho_{M^E}^{\pi_{M^E}^{\text{soft}}} \right\|_1 \leq \frac{2}{1-\gamma} \max_s D_{\text{TV}} \left(\pi_{M^L}^{\text{soft}}(\cdot|s), \pi_{M^E}^{\text{soft}}(\cdot|s) \right)$$

Moreover, upper bounding the right hand side by Pinsker's inequality:

$$\left\| \rho_{M^E}^{\pi_{M^L}^{\text{soft}}} - \rho_{M^E}^{\pi_{M^E}^{\text{soft}}} \right\|_1 \leq \frac{2}{1-\gamma} \sqrt{2 \max_s D_{\text{KL}} \left(\pi_{M^L}^{\text{soft}}(\cdot|s), \pi_{M^E}^{\text{soft}}(\cdot|s) \right)} \tag{19}$$

It rests to bound the following KL-divergence for any s :

$$\begin{aligned}
D_{\text{KL}} \left(\pi_{M_{\theta^*}^L}^{\text{soft}}(\cdot|s), \pi_{M_{\theta^*}^E}^{\text{soft}}(\cdot|s) \right) &= \sum_a \pi_{M_{\theta^*}^L}^{\text{soft}}(a|s) \log \frac{\pi_{M_{\theta^*}^L}^{\text{soft}}(a|s)}{\pi_{M_{\theta^*}^E}^{\text{soft}}(a|s)} \\
&= \sum_a \frac{Z_{a|s}^L}{Z_s^L} \left(\log \frac{Z_{a|s}^L}{Z_{a|s}^E} + \log \frac{Z_s^E}{Z_s^L} \right) \\
&= \sum_a \frac{Z_{a|s}^L}{Z_s^L} \log \frac{Z_{a|s}^L}{Z_{a|s}^E} + \log \frac{Z_s^E}{Z_s^L}
\end{aligned} \tag{20}$$

By using the log-sum inequality on the term depending on the states only:

$$\begin{aligned}
\log \frac{Z_s^E}{Z_s^L} &= \underbrace{\sum_a \frac{Z_{a|s}^E}{Z_s^E}}_1 \log \frac{Z_s^E}{Z_s^L} \\
&= \sum_a \frac{Z_{a|s}^E}{Z_s^E} \log \frac{\sum_a Z_{a|s}^E}{\sum_a Z_{a|s}^L} \\
&\leq \frac{1}{Z_s^E} \sum_a Z_{a|s}^E \log \frac{Z_{a|s}^E}{Z_{a|s}^L}
\end{aligned} \tag{21}$$

⁶Notice that the bound in (18) holds also for the case of reward dependent on states only. Indeed,

$$\begin{aligned}
\left| V_{M_{\theta^*}^E}^{\pi_{M_{\theta^*}^L}^{\text{soft}}} - V_{M_{\theta^*}^E}^{\pi_{M_{\theta^*}^E}^{\text{soft}}} \right| &= \frac{1}{1-\gamma} \left| \sum_s \left(\rho_{M_{\theta^*}^E}^{\pi_{M_{\theta^*}^L}^{\text{soft}}}(s) - \rho_{M_{\theta^*}^E}^{\pi_{M_{\theta^*}^E}^{\text{soft}}}(s) \right) R_{\theta^*}(s) \right| = \\
\frac{1}{1-\gamma} \left| \sum_s \left(\sum_a \rho_{M_{\theta^*}^E}^{\pi_{M_{\theta^*}^L}^{\text{soft}}}(s,a) - \sum_a \rho_{M_{\theta^*}^E}^{\pi_{M_{\theta^*}^E}^{\text{soft}}}(s,a) \right) R_{\theta^*}(s) \right| &= \frac{1}{1-\gamma} \left| \sum_{s,a} \left(\rho_{M_{\theta^*}^E}^{\pi_{M_{\theta^*}^L}^{\text{soft}}}(s,a) - \rho_{M_{\theta^*}^E}^{\pi_{M_{\theta^*}^E}^{\text{soft}}}(s,a) \right) R_{\theta^*}(s) \right|.
\end{aligned}$$

Consequently, replacing (21) in (20), and using the definitions (14) and (16), we have:

$$\begin{aligned}
D_{\text{KL}}\left(\pi_{M_{\theta^*}^L}^{\text{soft}}(\cdot|s), \pi_{M_{\theta^*}^E}^{\text{soft}}(\cdot|s)\right) &\leq \sum_a \left(\frac{Z_{a|s}^L}{Z_s^L} - \frac{Z_{a|s}^E}{Z_s^E}\right) \log \frac{Z_{a|s}^L}{Z_{a|s}^E} \\
&= \sum_a \left(\pi_{M_{\theta^*}^L}^{\text{soft}}(a|s) - \pi_{M_{\theta^*}^E}^{\text{soft}}(a|s)\right) \log \frac{Z_{a|s}^L}{Z_{a|s}^E} \\
&\leq \sum_a \left|\pi_{M_{\theta^*}^L}^{\text{soft}}(a|s) - \pi_{M_{\theta^*}^E}^{\text{soft}}(a|s)\right| \left|\log \frac{Z_{a|s}^L}{Z_{a|s}^E}\right| \\
&\leq \sum_a \left|\pi_{M_{\theta^*}^L}^{\text{soft}}(a|s) - \pi_{M_{\theta^*}^E}^{\text{soft}}(a|s)\right| \max_a \left|\log \frac{Z_{a|s}^L}{Z_{a|s}^E}\right| \\
&= \left\|\pi_{M_{\theta^*}^L}^{\text{soft}}(a|s) - \pi_{M_{\theta^*}^E}^{\text{soft}}(a|s)\right\|_1 \max_a \left|\log \frac{Z_{a|s}^L}{Z_{a|s}^E}\right| \\
&\leq 2 \max_a \left|\log \frac{Z_{a|s}^L}{Z_{a|s}^E}\right|
\end{aligned}$$

Consequently:

$$\max_s D_{\text{KL}}\left(\pi_{M_{\theta^*}^L}^{\text{soft}}(\cdot|s), \pi_{M_{\theta^*}^E}^{\text{soft}}(\cdot|s)\right) \leq 2 \max_{s,a} \left|\log \frac{Z_{a|s}^L}{Z_{a|s}^E}\right| \quad (22)$$

Hence, we can further upper bound the RHS of (19) by upper bounding the RHS of (22). To this end, we exploit the following fact:

$$\max_{s,a} \left|\log \frac{Z_{a|s}^L}{Z_{a|s}^E}\right| = \max \left\{ \log \frac{Z_{\bar{a}|\bar{s}}^L}{Z_{\bar{a}|\bar{s}}^E}, \log \frac{Z_{\underline{a}|\underline{s}}^E}{Z_{\underline{a}|\underline{s}}^L} \right\}, \quad (23)$$

where we adopted the following notation:

$$(\bar{s}, \bar{a}) = \arg \max_{s,a} \log \frac{Z_{a|s}^L}{Z_{a|s}^E} \quad (24)$$

$$(\underline{s}, \underline{a}) = \arg \min_{s,a} \log \frac{Z_{a|s}^L}{Z_{a|s}^E} \quad (25)$$

At this point, we can bound separately the two arguments of the max in (23). Starting from (24):

$$\begin{aligned}
\log \frac{Z_{\bar{a}|\bar{s}}^L}{Z_{\bar{a}|\bar{s}}^E} &= \log Z_{\bar{a}|\bar{s}}^L - \log Z_{\bar{a}|\bar{s}}^E \\
&= \underbrace{R_{\theta^*}(\bar{s}, \bar{a}) - R_{\theta^*}(\bar{s}, \bar{a})}_0 + \gamma \left\{ \sum_{s'} T^L(s'|\bar{s}, \bar{a}) \log Z_{s'}^L - T^E(s'|\bar{s}, \bar{a}) \log Z_{s'}^E \right\} \\
&= \gamma \left\{ \sum_{s'} T^L(s'|\bar{s}, \bar{a}) \log \frac{Z_{s'}^L}{Z_{s'}^E} + (T^L(s'|\bar{s}, \bar{a}) - T^E(s'|\bar{s}, \bar{a})) \log Z_{s'}^E \right\} \\
&\leq \gamma \left\{ \sum_{s'} T^L(s'|\bar{s}, \bar{a}) \left(\sum_a \pi_{M_{\theta^*}^L}^{\text{soft}}(a|s') \log \frac{Z_{a|s'}^L}{Z_{a|s'}^E} \right) + (T^L(s'|\bar{s}, \bar{a}) - T^E(s'|\bar{s}, \bar{a})) \log Z_{s'}^E \right\} \\
&\leq \gamma \log \frac{Z_{\bar{a}|\bar{s}}^L}{Z_{\bar{a}|\bar{s}}^E} + \gamma \sum_{s'} (T^L(s'|\bar{s}, \bar{a}) - T^E(s'|\bar{s}, \bar{a})) \log Z_{s'}^E
\end{aligned}$$

By rearranging the terms, we get:

$$\log \frac{Z_{\bar{a}|\bar{s}}^L}{Z_{\bar{a}|\bar{s}}^E} \leq \frac{\gamma}{1-\gamma} \sum_{s'} (T^L(s'|\bar{s}, \bar{a}) - T^E(s'|\bar{s}, \bar{a})) \log Z_{s'}^E$$

$$\begin{aligned}
&\leq \frac{\gamma}{1-\gamma} \sum_{s'} |T^L(s'|\bar{s}, \bar{a}) - T^E(s'|\bar{s}, \bar{a})| |\log Z_{s'}^E| \\
&\leq \frac{\gamma}{1-\gamma} \max_{s'} |\log Z_{s'}^E| \sum_{s'} |T^L(s'|\bar{s}, \bar{a}) - T^E(s'|\bar{s}, \bar{a})| \tag{26}
\end{aligned}$$

Then, with analogous calculations for the second argument of the max operator in (23), we have

$$\begin{aligned}
\log \frac{Z_{\underline{a}|\underline{s}}^E}{Z_{\underline{a}|\underline{s}}^L} &= \log Z_{\underline{a}|\underline{s}}^E - \log Z_{\underline{a}|\underline{s}}^L \\
&= \underbrace{R_{\theta^*}(\underline{s}, \underline{a}) - R_{\theta^*}(\underline{s}, \underline{a})}_0 + \gamma \left\{ \sum_{s'} T^E(s'|\underline{s}, \underline{a}) \log Z_{s'}^E - T^L(s'|\underline{s}, \underline{a}) \log Z_{s'}^L \right\} \\
&= \gamma \left\{ \sum_{s'} T^E(s'|\underline{s}, \underline{a}) \log \frac{Z_{s'}^E}{Z_{s'}^L} + (T^E(s'|\underline{s}, \underline{a}) - T^L(s'|\underline{s}, \underline{a})) \log Z_{s'}^L \right\} \\
&\leq \gamma \log \frac{Z_{\underline{a}|\underline{s}}^E}{Z_{\underline{a}|\underline{s}}^L} + \gamma \sum_{s'} (T^E(s'|\underline{s}, \underline{a}) - T^L(s'|\underline{s}, \underline{a})) \log Z_{s'}^L
\end{aligned}$$

It follows that:

$$\begin{aligned}
\log \frac{Z_{\underline{a}|\underline{s}}^E}{Z_{\underline{a}|\underline{s}}^L} &\leq \frac{\gamma}{1-\gamma} \sum_{s'} (T^E(s'|\underline{s}, \underline{a}) - T^L(s'|\underline{s}, \underline{a})) \log Z_{s'}^L \\
&\leq \frac{\gamma}{1-\gamma} \sum_{s'} |T^E(s'|\underline{s}, \underline{a}) - T^L(s'|\underline{s}, \underline{a})| |\log Z_{s'}^L| \\
&\leq \frac{\gamma}{1-\gamma} \max_{s'} |\log Z_{s'}^L| \sum_{s'} |T^E(s'|\underline{s}, \underline{a}) - T^L(s'|\underline{s}, \underline{a})| \tag{27}
\end{aligned}$$

We can plug in the bounds found in (27) and (26) in (23):

$$\max_{s,a} \left| \log \frac{Z_{a|s}^L}{Z_{a|s}^E} \right| \leq \frac{\gamma}{1-\gamma} \max \left\{ \max_{s'} |\log Z_{s'}^E|, \max_{s'} |\log Z_{s'}^L| \right\} \max_{s,a} \sum_{s'} |T^E(s'|s, a) - T^L(s'|s, a)| \tag{28}$$

It still remains to bound the term $\max \{ \max_{s'} |\log Z_{s'}^E|, \max_{s'} |\log Z_{s'}^L| \}$. It can be done by a splitting procedure similar to the one in (23). Indeed:

$$\max_{s'} |\log Z_{s'}^E| = \max \left\{ \log Z_{\bar{s}}^E, \log \frac{1}{Z_{\underline{s}}^E} \right\} \tag{29}$$

where, changing the previous definitions of \bar{s} and \underline{s} , we set:

$$\bar{s} = \arg \max_s \log Z_s^E \tag{30}$$

$$\underline{s} = \arg \min_s \log Z_s^E \tag{31}$$

Starting from the first term in (29) and applying (15):

$$\begin{aligned}
\log Z_{\bar{s}}^E &= \log \sum_a Z_{a|\bar{s}}^E \\
&\leq \log \left(|\mathcal{A}| \max_a Z_{a|\bar{s}}^E \right) \\
&= \log |\mathcal{A}| + \log \max_a Z_{a|\bar{s}}^E \\
&= \log |\mathcal{A}| + \max_a \log Z_{a|\bar{s}}^E \tag{32}
\end{aligned}$$

where the last equality follows from the fact that \log is a monotonically increasing function. Furthermore, (30) implies that $\log Z_{s'}^E \leq \log Z_{\bar{s}}^E \quad \forall s' \in \mathcal{S}$:

$$\max_a \log Z_{a|\bar{s}}^E \leq \max_a \left(R_{\theta^*}(\bar{s}, a) + \gamma \log Z_{\bar{s}}^E \sum_{s'} T(s'|\bar{s}, a) \right)$$

$$\leq R_{\max} + \gamma \log Z_{\underline{s}}^E \quad (33)$$

In the last inequality we have used the quantity R_{\max} that satisfies $R_{\theta^*}(s, a) \leq R_{\max} \quad \forall (s, a) \in \mathcal{S} \times \mathcal{A}$. In a similar fashion, we will use R_{\min} such that $R_{\theta^*}(s, a) \geq R_{\min} \quad \forall (s, a) \in \mathcal{S} \times \mathcal{A}$. Finally, plugging (33) into (32), we get:

$$\log Z_{\underline{s}}^E \leq \frac{R_{\max} + \log |\mathcal{A}|}{1 - \gamma} \quad (34)$$

We can proceed bounding the second argument of the max operator in (29). To this scope, we observe that $\sum_a \frac{1}{|\mathcal{A}|} = 1$ and then we apply the log-sum inequality as follows:

$$\begin{aligned} \log \frac{1}{Z_{\underline{s}}^E} &= \sum_a \frac{1}{|\mathcal{A}|} \log \frac{\sum_a \frac{1}{|\mathcal{A}|}}{\sum_a Z_{a|\underline{s}}^E} \\ &\leq \sum_a \frac{1}{|\mathcal{A}|} \log \frac{\frac{1}{|\mathcal{A}|}}{Z_{a|\underline{s}}^E} \\ &= \log \frac{1}{|\mathcal{A}|} + \sum_a \frac{1}{|\mathcal{A}|} \log \frac{1}{Z_{a|\underline{s}}^E} \\ &\leq \log \frac{1}{|\mathcal{A}|} + \max_a \log \frac{1}{Z_{a|\underline{s}}^E} \end{aligned} \quad (35)$$

Similarly to (33), we can apply one step of the soft Bellman equation to bound the term $\log \frac{1}{Z_{a|\underline{s}}^E}$:

$$\begin{aligned} \log \frac{1}{Z_{a|\underline{s}}^E} &= -\log Z_{a|\underline{s}}^E \\ &= -R_{\theta^*}(\underline{s}, a) - \gamma \sum_{s'} T^E(s'|\underline{s}, a) \log Z_{s'}^E \\ &= -R_{\theta^*}(\underline{s}, a) + \gamma \sum_{s'} T^E(s'|\underline{s}, a) \log \frac{1}{Z_{s'}^E} \\ &\leq -R_{\min} + \gamma \log \frac{1}{Z_{\underline{s}}^E} \underbrace{\sum_{s'} T^E(s'|\underline{s}, a)}_1 \end{aligned} \quad (36)$$

where in the last inequality we used (31), $R_{\theta^*}(s, a) \geq R_{\min} \quad \forall (s, a) \in \mathcal{S} \times \mathcal{A}$.

Since the upper bound in (36) does not depend on a :

$$\max_a \log \frac{1}{Z_{a|\underline{s}}^E} \leq -R_{\min} + \gamma \log \frac{1}{Z_{\underline{s}}^E} \quad (37)$$

Replacing (37) into (35), we have:

$$\log \frac{1}{Z_{\underline{s}}^E} \leq \log \frac{1}{|\mathcal{A}|} - R_{\min} + \gamma \log \frac{1}{Z_{\underline{s}}^E}$$

and consequently:

$$\log \frac{1}{Z_{\underline{s}}^E} \leq \frac{-\log |\mathcal{A}| - R_{\min}}{1 - \gamma} \quad (38)$$

Finally, using (34) and (38) in (29):

$$\max_{s'} |\log Z_{s'}^E| \leq \frac{1}{1 - \gamma} \max \{R_{\max} + \log |\mathcal{A}|, -\log |\mathcal{A}| - R_{\min}\} \quad (39)$$

In addition, one can notice that the bound (39) holds also for $\max_{s'} |\log Z_{s'}^L|$:

$$\max_{s'} |\log Z_{s'}^L| \leq \frac{1}{1 - \gamma} \max \{R_{\max} + \log |\mathcal{A}|, -\log |\mathcal{A}| - R_{\min}\}$$

So we can finally replace (39) in (28) that gives:

$$\max_{s,a} \left| \log \frac{Z_{a|s}^L}{Z_{a|s}^E} \right| \leq \frac{\gamma}{(1-\gamma)^2} \max \{R_{\max} + \log |\mathcal{A}|, -\log |\mathcal{A}| - R_{\min}\} \max_{s,a} \sum_{s'} |T^E(s'|s, a) - T^L(s'|s, a)| \quad (40)$$

We simplify the notation by introducing the constant C such that:

$$C := \sqrt{\gamma \max \{R_{\max} + \log |\mathcal{A}|, -\log |\mathcal{A}| - R_{\min}\}}$$

We can now go back through the inequality chain to eventually state the bound in the Theorem. First, plugging in (40) into (22) gives:

$$\max_s D_{\text{KL}} \left(\pi_{M_{\theta^*}^L}^{\text{soft}}(\cdot|s), \pi_{M_{\theta^*}^E}^{\text{soft}}(\cdot|s) \right) \leq \frac{2}{(1-\gamma)^2} C^2 \max_{s,a} \sum_{s'} |T^E(s'|s, a) - T^L(s'|s, a)| \quad (41)$$

Then, using (41) in (19) we have:

$$\left\| \rho_{M_{\theta^*}^L}^{\pi_{M_{\theta^*}^L}^{\text{soft}}} - \rho_{M_{\theta^*}^E}^{\pi_{M_{\theta^*}^E}^{\text{soft}}} \right\|_1 \leq \frac{2}{1-\gamma} \sqrt{\frac{4}{(1-\gamma)^2} C^2 \max_{s,a} \sum_{s'} |T^E(s'|s, a) - T^L(s'|s, a)|} \quad (42)$$

Finally, we arrive at the Theorem statement by replacing (42) in (18) and pulling the max operator out from the square root (using the fact that square root is monotonically increasing):

$$\left| V_{M_{\theta^*}^L}^{\pi_{M_{\theta^*}^L}^{\text{soft}}} - V_{M_{\theta^*}^E}^{\pi_{M_{\theta^*}^E}^{\text{soft}}} \right| \leq \frac{4CR_{\max}^{\text{abs}}}{(1-\gamma)^3} \max_{s,a} \sqrt{\sum_{s'} |T^E(s'|s, a) - T^L(s'|s, a)|} \quad (43)$$

□

C.2 Simulation Lemma for Occupancy Measures

Before moving to the proof of Theorem 2, we need a bound on the difference between the state occupancy measures attained by the same policy in MDPs with different transition dynamics measured in ℓ_1 -distance. This result can be obtained by adapting the Simulation Lemma for total expected return presented in [42] as expressed by the following Theorem.

Theorem 4. Consider $M_{\theta^*}^L$ and $M_{\theta^*}^E$. Then any policy π induces occupancy measures on the environments $M_{\theta^*}^L$ and $M_{\theta^*}^E$, respectively denoted as $\rho_{M^L}^\pi$ and $\rho_{M^E}^\pi$ that satisfy the following bound:

$$\|\rho_{M^L}^\pi - \rho_{M^E}^\pi\|_1 \leq \frac{\gamma}{(1-\gamma)} \mathbb{E}_{s' \sim \rho_{M^L}^\pi, a' \sim \pi} [\|T^L(\cdot|s', a') - T^E(\cdot|s', a')\|_1]$$

and consequently:

$$\|\rho_{M^L}^\pi - \rho_{M^E}^\pi\|_1 \leq \frac{\gamma}{(1-\gamma)} \max_{s', a'} \|T^L(\cdot|s', a') - T^E(\cdot|s', a')\|_1$$

Proof. We prove the result for the norm of the difference of the state-action occupancy measures that upper bounds the norm of the difference of the state only occupancy measures. Indeed:

$$\begin{aligned} \sum_s |\rho_{M^L}^\pi(s) - \rho_{M^E}^\pi(s)| &= \sum_s \left| \sum_a \rho_{M^L}^\pi(s, a) - \sum_a \rho_{M^E}^\pi(s, a) \right| \\ &= \sum_s \left| \sum_a (\rho_{M^L}^\pi(s, a) - \rho_{M^E}^\pi(s, a)) \right| \\ &\leq \sum_s \sum_a |\rho_{M^L}^\pi(s, a) - \rho_{M^E}^\pi(s, a)| \end{aligned}$$

First, notice that the occupancy measure ρ_M^π of a policy π in an MDP M with transition dynamics T is a stationary quantity. Consequently, for any state action pair the occupancy measure flux flowing

into the state minus the occupancy measure flux from that state is equal to zero. In addition, when a discounted problem is considered, the discount factor γ assumes the meaning of probability to continue the episode with another step towards another state. Consequently, $1 - \gamma$ represents the probability that the episode ends in the current state. Also this fact has to be taken into account in a discounted task. It follows that:

$$\underbrace{P_0(s)\pi(a|s)}_{\text{initial prob.}} + \underbrace{\gamma \sum_{s',a'} \rho_M^\pi(s',a')T(s|s',a')\pi(a|s)}_{\text{Incoming flux}} - \underbrace{\gamma \sum_{s',a'} \rho_M^\pi(s,a)T(s'|s,a)\pi(a'|s')}_{\text{Outcoming flux}} - \underbrace{\rho_M^\pi(s,a)(1-\gamma)}_{\text{Termination probability}} = 0$$

By normalization of probabilities in the second term:

$$P_0(s)\pi(a|s) + \gamma \sum_{s',a'} \rho_M^\pi(s',a')T(s|s',a')\pi(a|s) - \gamma \rho_M^\pi(s,a) - \rho_M^\pi(s,a)(1-\gamma) = 0$$

that implies:

$$\rho_M^\pi(s,a) = P_0(s)\pi(a|s) + \gamma \sum_{s',a'} \rho_M^\pi(s',a')T(s|s',a')\pi(a|s)$$

Notice the similarity to the Bellman equations.

Now, this result can be used to bound the difference between the occupancy measures induced by the same policy into the different environments $M_{\theta^*}^L$ and $M_{\theta^*}^E$. Indeed,

$$\begin{aligned} & \|\rho_{M^L}^\pi - \rho_{M^E}^\pi\|_1 \\ &= \gamma \sum_{s,a} \left| \sum_{s',a'} \rho_{M^L}^\pi(s',a')T^L(s|s',a')\pi(a|s) - \sum_{s',a'} \rho_{M^E}^\pi(s',a')T^E(s|s',a')\pi(a|s) \right|_1 \\ &= \gamma \sum_{s,a} |\pi(a|s)| \left| \sum_{s',a'} \rho_{M^L}^\pi(s',a')T^L(s|s',a') - \sum_{s',a'} \rho_{M^E}^\pi(s',a')T^E(s|s',a') \right| \\ &\stackrel{\text{a}}{\leq} \gamma \left\| \sum_{s',a'} \rho_{M^L}^\pi(s',a')T^L(\cdot|s',a') - \sum_{s',a'} \rho_{M^E}^\pi(s',a')T^E(\cdot|s',a') \right\|_1 \\ &\stackrel{\text{b}}{\leq} \gamma \left\| \sum_{s',a'} \rho_{M^L}^\pi(s',a') (T^L(\cdot|s',a') - T^E(\cdot|s',a')) \right\|_1 + \gamma \left\| \sum_{s',a'} T^E(\cdot|s',a') (\rho_{M^L}^\pi(s',a') - \rho_{M^E}^\pi(s',a')) \right\|_1 \\ &\leq \gamma \sum_{s',a'} \sum_s |\rho_{M^L}^\pi(s',a') (T^L(s|s',a') - T^E(s|s',a'))| + \gamma \sum_{s',a'} \sum_s |T^E(s|s',a') (\rho_{M^L}^\pi(s',a') - \rho_{M^E}^\pi(s',a'))| \\ &= \gamma \sum_{s',a'} \rho_{M^L}^\pi(s',a') \|T^L(\cdot|s',a') - T^E(\cdot|s',a')\|_1 + \gamma \sum_{s',a'} |\rho_{M^L}^\pi(s',a') - \rho_{M^E}^\pi(s',a')| \underbrace{\sum_s T^E(s|s',a')}_{=1} \\ &= \gamma \mathbb{E}_{s',a' \sim \rho_{M^L}^\pi} [\|T^L(\cdot|s',a') - T^E(\cdot|s',a')\|_1] + \gamma \|\rho_{M^L}^\pi - \rho_{M^E}^\pi\|_1 \end{aligned}$$

where in inequality a we used $\pi(a|s) \leq 1$, and in b we add and subtract inside the sum $\rho_{M^L}^\pi(s',a')T^E(\cdot|s',a')$ and then we use triangular inequality. The result presented in Theorem 4 is obtained bringing on the LHS the second term of the latest expression:

$$\|\rho_{M^L}^\pi - \rho_{M^E}^\pi\|_1 \leq \frac{\gamma}{(1-\gamma)} \mathbb{E}_{s',a' \sim \rho_{M^L}^\pi} [\|T^L(\cdot|s',a') - T^E(\cdot|s',a')\|_1]$$

□

C.3 Proof of Theorem 2

Proof. In this proof, the occupancy measures are state only occupancy measures. Thanks to (18) applied in the case of rewards depending solely on the states, we can state that:

$$\left| V_{M_{\theta^*}^L}^{\text{soft}} - V_{M_{\theta^*}^E}^{\text{soft}} \right| \leq \frac{P_{\max}^{\text{abs}}}{1-\gamma} \left\| \rho_{M_{\theta^*}^L}^{\text{soft}} - \rho_{M_{\theta^*}^E}^{\text{soft}} \right\|_1$$

Then using triangular inequality on the RHS we can write:

$$\left\| \begin{matrix} \pi_{M\theta}^{\text{soft}} \\ \rho_{M^L} \end{matrix} - \begin{matrix} \pi_{M\theta^E}^{\text{soft}} \\ \rho_{M^L} \end{matrix} \right\|_1 \leq \left\| \begin{matrix} \pi_{M\theta}^{\text{soft}} \\ \rho_{M^L} \end{matrix} - \begin{matrix} \pi_{M\theta^*}^{\text{soft}} \\ \rho_{M^L} \end{matrix} \right\|_1 + \left\| \begin{matrix} \pi_{M\theta^*}^{\text{soft}} \\ \rho_{M^L} \end{matrix} - \begin{matrix} \pi_{M\theta^*}^{\text{soft}} \\ \rho_{M^E} \end{matrix} \right\|_1 + \left\| \begin{matrix} \pi_{M\theta^*}^{\text{soft}} \\ \rho_{M^E} \end{matrix} - \begin{matrix} \pi_{M\theta^E}^{\text{soft}} \\ \rho_{M^L} \end{matrix} \right\|_1$$

However, the first term vanishes because the policy $\pi_{M\theta}^{\text{soft}}$ is the solution to the optimization problem

(1)-(2) when when we use $\rho_{M^L}^{\pi_{M\theta^*}^{\text{soft}}}$ as ρ in (2). Analogously, the policy $\pi_{M\theta^E}^{\text{soft}}$ is the solution to the

optimization problem (1)-(2) when when we use $\rho_{M^E}^{\pi_{M\theta^*}^{\text{soft}}}$ as ρ in (2). Hence, the third term is also zero. Canceling the vanishing terms, we obtain:

$$\left| V_{M\theta^*}^{\pi_{M\theta}^{\text{soft}}} - V_{M\theta^*}^{\pi_{M\theta^E}^{\text{soft}}} \right| \leq \frac{R_{\max}^{\text{abs}}}{1-\gamma} \left\| \begin{matrix} \pi_{M\theta^*}^{\text{soft}} \\ \rho_{M^L} \end{matrix} - \begin{matrix} \pi_{M\theta^*}^{\text{soft}} \\ \rho_{M^E} \end{matrix} \right\|_1$$

Then, adding and subtracting $\rho_{M^E}^{\pi_{M\theta^*}^{\text{soft}}}$ and taking again advantage of triangular inequality in the RHS we have:

$$\left| V_{M\theta^*}^{\pi_{M\theta}^{\text{soft}}} - V_{M\theta^*}^{\pi_{M\theta^E}^{\text{soft}}} \right| \leq \frac{R_{\max}^{\text{abs}}}{1-\gamma} \left[\left\| \begin{matrix} \pi_{M\theta^*}^{\text{soft}} \\ \rho_{M^L} \end{matrix} - \begin{matrix} \pi_{M\theta^*}^{\text{soft}} \\ \rho_{M^E} \end{matrix} \right\|_1 + \left\| \begin{matrix} \pi_{M\theta^*}^{\text{soft}} \\ \rho_{M^E} \end{matrix} - \begin{matrix} \pi_{M\theta^*}^{\text{soft}} \\ \rho_{M^E} \end{matrix} \right\|_1 \right]$$

Finally, bounding the second term with the bound in Theorem 1 and the first one with the Simulation Lemma 4 yields the result. \square

C.4 Proof of Theorem 3

C.4.1 Impossibility to match the State-action Occupancy Measure

Before proving the theorem, we show that finding the policy $\pi^*(a|s)$ whose state-action occupancy measure matches the state-action visitation frequency ρ of the expert⁷ is impossible in case of model mismatch. Consider:

$$\begin{aligned} \rho(s, a) &= \rho_{M^L}^{\pi^*}(s, a) \\ \rho(s)\pi^E(a|s) &= \rho_{M^L}^{\pi^*}(s)\pi^*(a|s) \\ \pi^*(a|s) &= \pi^E(a|s) \frac{\rho(s)}{\rho_{M^L}^{\pi^*}(s)} \end{aligned}$$

Notice that the policy π^* does not sum to one, when there is model mismatch, i.e., the feasible set of (1)-(2) would be empty if state-action occupancy measures were used in posing the constraint (2). In addition, even if the two environments were the same, only the expert policy would have been in the feasible set because there exists an injective mapping from state-action visitation frequencies to policies as already noted in [31, 43].

C.4.2 Theorem Proof

Proof. If there exists a policy π^* that matches the expert occupancy measure $\rho(s)$ in the environment M_{θ}^L , the Bellman flow constraints [43] leads to the following equation for each state $s \in \mathcal{S}$:

$$\rho(s) - P_0(s) = \gamma \sum_{s', a'} \rho(s') \pi^*(a'|s') T^L(s|s', a') \quad (44)$$

This can be seen by writing the Bellman flow constraints for the expert policy π^E with transition dynamics T^E , and for the policy π^* with transition dynamics T^L :

$$\rho(s) - P_0(s) = \gamma \sum_{s', a'} \rho(s') \pi^E(a'|s') T^E(s|s', a') \quad (45)$$

⁷In this proof the expert policy is denoted by π^E . In the specific case of our paper it stands for either $\pi_{M\theta}^{\text{soft}}$ or $\pi_{M\theta^E}^{\text{soft}}$. However, the result holds for every valid expert policy.

$$\rho_{M^L}^{\pi^*}(s) - P_0(s) = \gamma \sum_{s', a'} \rho_{M^L}^{\pi^*}(s') \pi^*(a'|s') T^L(s|s', a') \quad (46)$$

By definition of π^* , the two occupancy measures are equal, so we can equate the LHS of (45) to the RHS of (46), obtaining:

$$\rho(s) - P_0(s) = \gamma \sum_{s', a'} \rho_{M^L}^{\pi^*}(s') \pi^*(a'|s') T^L(s|s', a')$$

Finally, replacing ρ in the RHS, one obtains the equation in (44). In addition, for each state we have the condition on the normalization of the policy:

$$1 = \sum_a \pi^*(a|s), \quad \forall s \in \mathcal{S}$$

All these conditions can be seen as an underdetermined system with $2|\mathcal{S}|$ equations ($|\mathcal{S}|$ for normalization, and $|\mathcal{S}|$ for the Bellman flow constraints). The unknown is the policy π^* represented by the $|\mathcal{S}| \times |\mathcal{A}|$ entries of the vector π^* .

We introduce the matrix \mathbf{T} . In the first $|\mathcal{S}|$ rows, the entry in the s^{th} row and $(s'|\mathcal{A}| + a')^{\text{th}}$ column is the element $\rho(s')T^L(s|s', a')$. In the last $|\mathcal{S}|$ rows, the entries are instead given by 1 from position $s'|\mathcal{A}|$ to position $s'|\mathcal{A}| + |\mathcal{A}|$. These rows of the matrix serves to impose the normalization condition for each possible state.

We can thus write the underdetermined system as:

$$\begin{bmatrix} \rho - P_0 \\ \mathbf{1}_{|\mathcal{S}|} \end{bmatrix} = \mathbf{T} \pi^*, \quad (47)$$

where the left hand side is a vector whose first $|\mathcal{S}|$ positions are the element-wise difference between the state occupancy measure and the initial probability distribution for each state, and the second half are all ones. The right hand side is instead written using the matrix \mathbf{T} , and the optimal policy vector π^* , that are more precisely described in (48) and (49) respectively.

If we look at the dimensions we notice that in the left hand side we have $2|\mathcal{S}|$ conditions, so the rank of the matrix \mathbf{T} has to be at least $2|\mathcal{S}|$ to guarantee that the system admits infinitely many solutions for π^* . Considering that \mathbf{T} has $2|\mathcal{S}|$ rows, its rank is at most $2|\mathcal{S}|$. Consequently, we need to require full-rank for \mathbf{T} . This fact limits the class of perturbation in the dynamics that can be considered still achieving perfect matching. In the following two paragraphs, we provide a more visual description of the quantities appearing in the right hand side of the system (47).

Block Representation of the Matrix \mathbf{T} . We can define, for each state $s \in \mathcal{S}$, the probability flows matrix $\mathbf{F}(s) \in \mathbb{R}^{|\mathcal{S}| \times |\mathcal{A}|}$ as follows:

$$\mathbf{F}(s) = \begin{bmatrix} \rho(s)T^L(s_1|s, a_1) & \rho(s)T^L(s_1|s, a_2) & \dots & \rho(s)T^L(s_1|s, a_{|\mathcal{A}|}) \\ \rho(s)T^L(s_2|s, a_1) & \rho(s)T^L(s_2|s, a_2) & \dots & \rho(s)T^L(s_2|s, a_{|\mathcal{A}|}) \\ \vdots & \vdots & \ddots & \vdots \\ \rho(s)T^L(s_{|\mathcal{S}}|s, a_1) & \rho(s)T^L(s_{|\mathcal{S}}|s, a_2) & \dots & \rho(s)T^L(s_{|\mathcal{S}}|s, a_{|\mathcal{A}|}) \end{bmatrix}$$

Then, we define the unitary row matrix $\mathbf{B}(s) \in \mathbb{R}^{|\mathcal{S}| \times |\mathcal{A}|}$ to be zero everywhere, but in row s that contains only ones. It has a number of columns equal to the cardinality of the action space \mathcal{A} . For example, when $|\mathcal{A}| = 4$ and $|\mathcal{S}| = 6$, the unitary row matrix for the state s_3 is:

$$\mathbf{B}(s_3) = \begin{bmatrix} 0 & 0 & 0 & 0 \\ 0 & 0 & 0 & 0 \\ 1 & 1 & 1 & 1 \\ 0 & 0 & 0 & 0 \\ 0 & 0 & 0 & 0 \\ 0 & 0 & 0 & 0 \end{bmatrix}$$

Then, we can represent the matrix $\mathbf{T} \in \mathbb{R}^{2|\mathcal{S}| \times |\mathcal{S}||\mathcal{A}|}$ by stacking unitaries and probability flows matrices in the following fashion:

$$\mathbf{T} = \begin{bmatrix} \mathbf{F}(s_1) & \mathbf{F}(s_2) & \dots & \mathbf{F}(s_{|\mathcal{S}|}) \\ \mathbf{B}(s_1) & \mathbf{B}(s_2) & \dots & \mathbf{B}(s_{|\mathcal{S}|}) \end{bmatrix} \quad (48)$$

Block Representation of the Optimal Policy Vector π^* . For each state $s \in \mathcal{S}$, we can define a local optimal policy vector $\pi^*(s) \in \mathbb{R}^{|\mathcal{A}|}$ as:

$$\pi^*(s) = \begin{bmatrix} \pi(a_1|s) \\ \pi(a_2|s) \\ \vdots \\ \pi(a_{|\mathcal{A}|}|s) \end{bmatrix}$$

Then, the optimal policy vector $\pi^* \in \mathbb{R}^{|\mathcal{S}||\mathcal{A}|}$ is given by the vertical stacking of the local optimal vectors:

$$\pi^* = \begin{bmatrix} \pi^*(s_1) \\ \pi^*(s_2) \\ \vdots \\ \pi^*(s_{|\mathcal{S}|}) \end{bmatrix} \quad (49)$$

□

D Deriving Gradient-based Method from Worst-case Predictive Log-loss

We consider again in this section the optimization problem given in (1)-(2) with model mismatch, i.e., using $\rho_{M^E}^{\pi_{M^E}^{\text{soft}}}$ as ρ . The aim of this section is to give an alternative point of view on this program based on a proper adaptation of the worst-case predictive log-loss [23, Corollary 6.3] to the model mismatch case.

[23] proved that the maximum causal entropy policy satisfying the optimization constraints is also the distribution that minimizes the worst-case predictive log-loss. However, the proof leverages on the fact that learner and expert MDPs coincide, an assumption that fails in the scenario of our work.

This section extends the result to the general case, where expert and learner MDP do not coincide, thanks to the two following contributions: (i) we show that the MCE constrained maximization given in (4)-(5) in the main text can be recast as a worst-case predictive log-loss constrained minimization and (ii) that this alternative problem leads to the same reward weights update found in the main text for the dual of the program (4)-(5). We start reporting again the optimization problem of interest:

$$\arg \max_{\pi \in \Pi} \mathbb{E} \left[\sum_{t=0}^{\infty} -\gamma^t \log \pi(a_t|s_t) \mid \pi, M^L \right] \quad (50)$$

$$\text{subject to } \rho_{M^E}^{\pi_{M^E}^{\text{soft}}} = \rho_{M^L}^{\pi} \quad (51)$$

An alternative interpretation of the entropy is given by the following property:

$$\mathbb{E} \left[\sum_{t=0}^{\infty} -\gamma^t \log \pi(a_t|s_t) \mid \pi, M^L \right] = \inf_{\tilde{\pi}} \mathbb{E} \left[\sum_{t=0}^{\infty} -\gamma^t \log \tilde{\pi}(a_t|s_t) \mid \pi, M^L \right], \quad \forall \pi$$

Thus, it holds also for $\pi_{M^E}^{\text{soft}}$ solution of the primal optimization problem (50)- (51), that exists if Theorem 3 is satisfied. In addition, to maintain the equivalence with the program (50)-(51), we restrict the inf search space to the feasible set of (50)-(51) that we denote $\tilde{\Pi}$.

$$\mathbb{E} \left[\sum_{t=0}^{\infty} -\gamma^t \log \pi_{M^E}^{\text{soft}}(a_t|s_t) \mid \pi_{M^E}^{\text{soft}}, M^L \right] = \inf_{\tilde{\pi} \in \tilde{\Pi}} \mathbb{E} \left[\sum_{t=0}^{\infty} -\gamma^t \log \tilde{\pi}(a_t|s_t) \mid \pi_{M^E}^{\text{soft}}, M^L \right]$$

Notice that since $\pi_{M^E}^{\text{soft}}$ is solution of the maximization problem, we can indicate the the previous equality as:

$$\sup_{\tilde{\pi} \in \tilde{\Pi}} \mathbb{E} \left[\sum_{t=0}^{\infty} -\gamma^t \log \tilde{\pi}(a_t|s_t) \mid \tilde{\pi}, M^L \right] = \inf_{\tilde{\pi} \in \tilde{\Pi}} \sup_{\tilde{\pi} \in \tilde{\Pi}} \mathbb{E} \left[\sum_{t=0}^{\infty} -\gamma^t \log \tilde{\pi}(a_t|s_t) \mid \tilde{\pi}, M^L \right] \quad (52)$$

It is thus natural to interpret the quantity:

$$c(\pi) = \mathbb{E} \left[\sum_{t=0}^{\infty} -\gamma^t \log \pi(a_t | s_t) \mid \pi_{M_{\theta E}^{\text{soft}}}, M^L \right] \quad (53)$$

as the cost function associated to the policy π because, according to (52), this quantity is equivalent to the worst-case predictive log-loss among the policies of the feasible set $\tilde{\Pi}$. It can be seen that the loss inherits the feasible set of the original MCE maximization problem as search space for the inf and sup operations. It follows that in case of model mismatch, the loss studied in [23, Corollary 6.3] is modified because a different set must be used as search space for the inf and sup.

In the following, we develop a gradient based method to minimize this cost and, thus, the worst case predictive log-loss.⁸

Furthermore, we can already consider that π belongs to the family of soft Bellman policies parametrized by the parameter θ in the environment M_{θ}^L because they are the family of distributions attaining maximum discounted causal entropy (*cf.*, [31, Lemma 3]). The cost is, in this case, expressed for the parameter θ :

$$c(\theta) = \mathbb{E} \left[\sum_{t=0}^{\infty} -\gamma^t \log \pi_{M_{\theta}^{\text{soft}}}^{\text{soft}}(a_t | s_t) \mid \pi_{M_{\theta E}^{\text{soft}}}, M^L \right] \quad (54)$$

Theorem 5. *If $\pi_{M_{\theta E}^{\text{soft}}}$ exists, the gradient of the cost function given in (54) is equal to:*

$$\nabla_{\theta} c(\theta) = \sum_s \left(\rho_{M_L}^{\pi_{M_{\theta}^{\text{soft}}}}(s) - \rho_{M_E}^{\pi_{M_{\theta E}^{\text{soft}}}}(s) \right) \nabla_{\theta} R_{\theta}(s)$$

In addition, this result generalizes when the expectation in the cost function is taken with respect to any of the policies in the feasible set of the primal problem (50)-(51).

Note that choosing one-hot features, we have $\nabla_{\theta} c(\theta) = \rho_{M_L}^{\pi_{M_{\theta}^{\text{soft}}}} - \rho_{M_E}^{\pi_{M_{\theta E}^{\text{soft}}}}$ as used in Section 4.

Uniqueness of the Solution. The cost in equation (54) is strictly convex in the soft max policy $\pi_{M_{\theta}^{\text{soft}}}$ because $-\log(\cdot)$ is a strictly convex function and the cost consists in a linear composition of these strictly convex functions. Thus the gradient descent converges to a unique soft optimal policy. In addition, the fact that for each possible θ , the quantity $\log \pi_{M_{\theta}^{\text{soft}}} = Q_{M_{\theta}}^{\text{soft}}(s, a) - V_{M_{\theta}}^{\text{soft}}(s)$ is convex in θ since the soft value functions ($Q_{M_{\theta}}^{\text{soft}}(s, a)$ and $V_{M_{\theta}}^{\text{soft}}(s)$) are given by a sum of rewards that are linear in θ and LogSumExp functions that are convex. It follows that $\log \pi_{M_{\theta}^{\text{soft}}}$ is a composition of linear and convex functions for each state actions pairs. Consequently the cost given in (54) is convex in θ . It follows that alternating an update of the parameter θ using a gradient descent scheme based on the gradient given by Theorem 5 with a derivation of the corresponding soft-optimal policy by Soft-Value-Iteration, one can converge to θ_E whose corresponding soft optimal policy is $\pi_{M_{\theta E}^{\text{soft}}}$. However, considering that the function LogSumExp is convex but not strictly convex there is no unique θ_E corresponding to the soft optimal policy $\pi_{M_{\theta E}^{\text{soft}}}$.

D.1 Proof of Theorem 5

Proof. We will make use of the following quantities:

- $P_t^{\pi_{M_{\theta}^{\text{soft}}}}(s)$ defined as the probability of visiting state s at time t by the policy $\pi_{M_{\theta}^{\text{soft}}}$ acting in M_{θ}^L

⁸If we used $\rho_{M^L}^{\pi_{M_{\theta}^{\text{soft}}}}$ as ρ , we would have obtained the cost $c(\pi) = \mathbb{E} \left[\sum_{t=0}^{\infty} -\gamma^t \log \pi(a_t | s_t) \mid \pi_{M_{\theta}^{\text{soft}}}, M^L \right]$.

In this case, the gradient is known see [44].

- $P_t^{\pi_{M_\theta^L}^{\text{soft}}}(s, a)$ defined as the probability of visiting state s and taking action a from state s at time t by the policy $\pi_{M_\theta^L}^{\text{soft}}$ acting in M_θ^L
- $P_t^{\pi_{M_{\theta E}^L}^{\text{soft}}}(s)$ defined as the probability of visiting state s at time t by the policy $\pi_{M_{\theta E}^L}^{\text{soft}}$ acting in $M_{\theta E}^L$
- $P_t^{\pi_{M_{\theta E}^L}^{\text{soft}}}(s, a)$ defined as the probability of visiting state s and taking action a from state s at time t by the policy $\pi_{M_{\theta E}^L}^{\text{soft}}$ acting in $M_{\theta E}^L$

The cost can be rewritten as:

$$\begin{aligned}
c(\theta) &= - \sum_{t=0}^{\infty} \gamma^t \sum_{s \in \mathcal{S}} \sum_{a \in \mathcal{A}} P_t^{\pi_{M_{\theta E}^L}^{\text{soft}}}(s, a) \log \pi_{M_\theta^L}^{\text{soft}}(a|s) \\
&= - \sum_{s \in \mathcal{S}} \sum_{a \in \mathcal{A}} P_0^{\pi_{M_{\theta E}^L}^{\text{soft}}}(s, a) \left(Q_{M_\theta^L}^{\text{soft}}(s, a) - V_{M_\theta^L}^{\text{soft}}(s) \right) \\
&\quad - \sum_{s \in \mathcal{S}} \sum_{a \in \mathcal{A}} P_1^{\pi_{M_{\theta E}^L}^{\text{soft}}}(s, a) \gamma \left(Q_{M_\theta^L}^{\text{soft}}(s, a) - V_{M_\theta^L}^{\text{soft}}(s) \right) \\
&\quad - \sum_{s \in \mathcal{S}} \sum_{a \in \mathcal{A}} P_2^{\pi_{M_{\theta E}^L}^{\text{soft}}}(s, a) \gamma^2 \left(Q_{M_\theta^L}^{\text{soft}}(s, a) - V_{M_\theta^L}^{\text{soft}}(s) \right) \\
&\quad - \sum_{s \in \mathcal{S}} \sum_{a \in \mathcal{A}} P_3^{\pi_{M_{\theta E}^L}^{\text{soft}}}(s, a) \gamma^3 \left(Q_{M_\theta^L}^{\text{soft}}(s, a) - V_{M_\theta^L}^{\text{soft}}(s) \right) \\
&\quad \dots \\
&= \sum_{s, a} P_0(s) \pi_{M_{\theta E}^L}^{\text{soft}}(a|s) V_{M_\theta^L}^{\text{soft}}(s) \tag{55}
\end{aligned}$$

$$- \sum_{s, a} P_0(s) \pi_{M_{\theta E}^L}^{\text{soft}}(a|s) Q_{M_\theta^L}^{\text{soft}}(s, a) + \gamma \sum_{s, a} P_1^{\pi_{M_{\theta E}^L}^{\text{soft}}}(s) \pi_{M_{\theta E}^L}^{\text{soft}}(a|s) V_{M_\theta^L}^{\text{soft}}(s) \tag{56}$$

$$- \gamma \sum_{s, a} P_1^{\pi_{M_{\theta E}^L}^{\text{soft}}}(s) \pi_{M_{\theta E}^L}^{\text{soft}}(a|s) Q_{M_\theta^L}^{\text{soft}}(s, a) + \gamma^2 \sum_{s, a} P_2^{\pi_{M_{\theta E}^L}^{\text{soft}}}(s) \pi_{M_{\theta E}^L}^{\text{soft}}(a|s) V_{M_\theta^L}^{\text{soft}}(s) \tag{57}$$

$$- \gamma^2 \sum_{s, a} P_2^{\pi_{M_{\theta E}^L}^{\text{soft}}}(s) \pi_{M_{\theta E}^L}^{\text{soft}}(a|s) Q_{M_\theta^L}^{\text{soft}}(s, a) + \gamma^3 \sum_{s, a} P_3^{\pi_{M_{\theta E}^L}^{\text{soft}}}(s) \pi_{M_{\theta E}^L}^{\text{soft}}(a|s) V_{M_\theta^L}^{\text{soft}}(s)$$

...

The gradient of the term in (55) has already been derived in [44] and it is given by:

$$\nabla_\theta \sum_{s, a} P_0(s) \pi_{M_{\theta E}^L}^{\text{soft}}(a|s) V_{M_\theta^L}^{\text{soft}}(s) = \nabla_\theta \sum_s P_0(s) V_{M_\theta^L}^{\text{soft}}(s) = \sum_{s, a} \rho_{M_\theta^L}^{\pi_{M_{\theta E}^L}^{\text{soft}}}(s, a) \nabla_\theta R_\theta(s, a)$$

Now, we compute the gradient of the following terms starting from (56). We notice that this term can be simplified as follows:

$$\begin{aligned}
&- \sum_{s, a} P_0(s) \pi_{M_{\theta E}^L}^{\text{soft}}(a|s) Q_{M_\theta^L}^{\text{soft}}(s, a) + \gamma \sum_{s, a} P_1^{\pi_{M_{\theta E}^L}^{\text{soft}}}(s) \pi_{M_{\theta E}^L}^{\text{soft}}(a|s) V_{M_\theta^L}^{\text{soft}}(s) \\
&= - \sum_{s, a} P_0(s) \pi_{M_{\theta E}^L}^{\text{soft}}(a|s) \left(R_\theta(s, a) + \gamma \sum_{s'} T^L(s'|s, a) V_{M_\theta^L}^{\text{soft}}(s') \right) + \gamma \sum_{s, a} P_1^{\pi_{M_{\theta E}^L}^{\text{soft}}}(s) \pi_{M_{\theta E}^L}^{\text{soft}}(a|s) V_{M_\theta^L}^{\text{soft}}(s)
\end{aligned}$$

$$\begin{aligned}
&= - \sum_{s,a} P_0(s) \pi_{M_{\theta E}^L}^{\text{soft}}(a|s) R_{\theta}(s,a) - \gamma \sum_{s'} \sum_{s,a} T^L(s'|s,a) P_0(s) \pi_{M_{\theta E}^L}^{\text{soft}}(a|s) V_{M_{\theta}^L}^{\text{soft}}(s') + \gamma \sum_s P_1^{\pi_{M_{\theta E}^L}^{\text{soft}}}(s) V_{M_{\theta}^L}^{\text{soft}}(s) \\
&= - \sum_{s,a} P_0(s) \pi_{M_{\theta E}^L}^{\text{soft}}(a|s) R_{\theta}(s,a) - \gamma \sum_{s'} P_1^{\pi_{M_{\theta E}^L}^{\text{soft}}}(s') V_{M_{\theta}^L}^{\text{soft}}(s') + \gamma \sum_s P_1^{\pi_{M_{\theta E}^L}^{\text{soft}}}(s) V_{M_{\theta}^L}^{\text{soft}}(s) \\
&= - \sum_{s,a} P_0(s) \pi_{M_{\theta E}^L}^{\text{soft}}(a|s) R_{\theta}(s,a)
\end{aligned}$$

With similar steps, all the terms except the first one are given by

$$- \sum_{t=0}^{\infty} \sum_{s,a} P_t^{\pi_{M_{\theta E}^L}^{\text{soft}}}(s,a) \gamma^t R_{\theta}(s,a) = - \sum_{s,a} \rho_{M_{\theta E}^L}^{\pi_{M_{\theta E}^L}^{\text{soft}}}(s,a) R_{\theta}(s,a)$$

If the reward is state only, then and we can marginalize the sum over the action and then exploiting the fact that $\pi_{M_{\theta E}^L}^{\text{soft}}$ is in the feasible set of the primal problem (50)-(51):

$$- \sum_{t=0}^{\infty} \sum_{s,a} P_t^{\pi_{M_{\theta E}^L}^{\text{soft}}}(s,a) \gamma^t R_{\theta}(s) = - \sum_s \rho_{M^L}^{\pi_{M_{\theta E}^L}^{\text{soft}}}(s) R_{\theta}(s) = - \sum_s \rho_{M^E}^{\pi_{M_{\theta}^*}^{\text{soft}}}(s) R_{\theta}(s)$$

It follows that the gradient of all the terms but the first term (55) is given by:

$$- \sum_s \rho_{M^E}^{\pi_{M_{\theta}^*}^{\text{soft}}}(s) R_{\theta}(s)$$

Finally, the proof is concluded by summing the latest result to the gradient of (55) that gives:

$$\nabla_{\theta} c(\theta) = \sum_s \left(\rho_{M^L}^{\pi_{M_{\theta}^L}^{\text{soft}}}(s) - \rho_{M^E}^{\pi_{M_{\theta}^*}^{\text{soft}}}(s) \right) \nabla_{\theta} R_{\theta}(s)$$

It can be noticed that the computation of this gradient exploits only the fact that $\pi_{M_{\theta E}^L}^{\text{soft}}$ is in the primal feasible set and not the fact that it maximizes the discounted causal entropy. It follows that all the policies in the primal feasible set share this gradient. This means that this gradients aim to move the learner policy towards the primal feasible set while the causal entropy is then maximized by Soft-Value-Iteration. \square

E Further Details of Section 4

Here, we prove that the optimization problem in (10) can be solved by the Algorithm 2. First of all, one can rewrite (10) as:

$$\mathbb{E}_{s \sim P_0} \left[\mathbb{E} \left[\sum_{t=0}^{\infty} \gamma^t \left\{ R_{\theta}(s_t) + H^{\pi^{\text{pl}}}(A | S = s_t) \right\} \middle| \pi^{\text{pl}}, \pi^{\text{op}}, M^{\text{two},L,\alpha}, s_0 = s \right] \right]$$

The quantity inside the expectation over P_0 is usually known as free energy, and for each state $s \in \mathcal{S}$, it is equal to:

$$F(\pi^{\text{pl}}, \pi^{\text{op}}, s) = \mathbb{E} \left[\sum_{t=0}^{\infty} \gamma^t \left\{ R_{\theta}(s_t) + H^{\pi^{\text{pl}}}(A | S = s_t) \right\} \middle| \pi^{\text{pl}}, \pi^{\text{op}}, M^{\text{two},L,\alpha}, s_0 = s \right]$$

Separating the first term of the sum over temporal steps, one can observe a recursive relation that is useful for the development of the algorithm:

$$\begin{aligned}
&F(\pi^{\text{pl}}, \pi^{\text{op}}, s) \\
&= R_{\theta}(s) + H^{\pi^{\text{pl}}}(A | S = s)
\end{aligned}$$

$$\begin{aligned}
& + \mathbb{E}_{a^{\text{pl}} \sim \pi^{\text{pl}}, a^{\text{op}} \sim \pi^{\text{op}}} \left[\mathbb{E}_{s' \sim T^{\text{two}, L, \alpha}(\cdot | s, a^{\text{pl}}, a^{\text{op}})} \left[\mathbb{E} \left[\sum_{t=1}^{\infty} \gamma^t \left\{ R_{\theta}(s_t) + H^{\pi^{\text{pl}}}(A | S = s_t) \right\} \middle| \pi^{\text{pl}}, \pi^{\text{op}}, M^{\text{two}, L, \alpha}, s_1 = s' \right] \right] \right] \\
& = R_{\theta}(s) + H^{\pi^{\text{pl}}}(A | S = s) \\
& + \gamma \mathbb{E}_{a^{\text{pl}} \sim \pi^{\text{pl}}, a^{\text{op}} \sim \pi^{\text{op}}} \left[\mathbb{E}_{s' \sim T^{\text{two}, L, \alpha}(\cdot | s, a^{\text{pl}}, a^{\text{op}})} \left[\mathbb{E} \left[\sum_{t=0}^{\infty} \gamma^t \left\{ R_{\theta}(s_t) + H^{\pi^{\text{pl}}}(A | S = s_t) \right\} \middle| \pi^{\text{pl}}, \pi^{\text{op}}, M^{\text{two}, L, \alpha}, s_0 = s' \right] \right] \right] \\
& = R_{\theta}(s) + H^{\pi^{\text{pl}}}(A | S = s) + \gamma \mathbb{E}_{a^{\text{pl}} \sim \pi^{\text{pl}}, a^{\text{op}} \sim \pi^{\text{op}}} \left[\mathbb{E}_{s' \sim T^{\text{two}, L, \alpha}(\cdot | s, a^{\text{pl}}, a^{\text{op}})} [F(\pi^{\text{pl}}, \pi^{\text{op}}, s')] \right] \\
& = \mathbb{E}_{a^{\text{pl}} \sim \pi^{\text{pl}}, a^{\text{op}} \sim \pi^{\text{op}}} \left[R_{\theta}(s) - \log \pi^{\text{pl}}(a^{\text{pl}} | s) + \gamma \mathbb{E}_{s' \sim T^{\text{two}, L, \alpha}(\cdot | s, a^{\text{pl}}, a^{\text{op}})} [F(\pi^{\text{pl}}, \pi^{\text{op}}, s')] \right]
\end{aligned}$$

Then, our aim is to find the saddle point:

$$V(s) = \max_{\pi^{\text{pl}}} \min_{\pi^{\text{op}}} F(\pi^{\text{pl}}, \pi^{\text{op}}, s)$$

and the policies attaining it. Define the joint quality function for a triplet $(s, a^{\text{pl}}, a^{\text{op}})$ as:

$$Q(s, a^{\text{pl}}, a^{\text{op}}) = R_{\theta}(s) + \gamma \mathbb{E}_{s' \sim T(\cdot | s, a^{\text{pl}}, a^{\text{op}})} [V(s')]$$

In a dynamic programming context, the previous equation gives the quality function based on the observed reward and the current estimate of the saddle point V . This is done by step (11) in the Algorithm 2. It remains now to motivate the update of the saddle point estimate V in (12). Consider:

$$\begin{aligned}
& \max_{\pi^{\text{pl}}} \min_{\pi^{\text{op}}} F(\pi^{\text{pl}}, \pi^{\text{op}}, s) \\
& = \max_{\pi^{\text{pl}}} \min_{\pi^{\text{op}}} \mathbb{E}_{a^{\text{pl}} \sim \pi^{\text{pl}}(\cdot | s), a^{\text{op}} \sim \pi^{\text{op}}(\cdot | s)} [Q(s, a^{\text{pl}}, a^{\text{op}}) - \log \pi^{\text{pl}}(a^{\text{pl}} | s)] \\
& = \max_{\pi^{\text{pl}}} \min_{\pi^{\text{op}}} \mathbb{E}_{a^{\text{pl}} \sim \pi^{\text{pl}}(\cdot | s)} \left[\mathbb{E}_{a^{\text{op}} \sim \pi^{\text{op}}(\cdot | s)} [Q(s, a^{\text{pl}}, a^{\text{op}}) - \log \pi^{\text{pl}}(a^{\text{pl}} | s) | a^{\text{pl}}] \right] \\
& = \max_{\pi^{\text{pl}}} \mathbb{E}_{a^{\text{pl}} \sim \pi^{\text{pl}}(\cdot | s)} \left[\min_{\pi^{\text{op}}} \mathbb{E}_{a^{\text{op}} \sim \pi^{\text{op}}(\cdot | s)} [Q(s, a^{\text{pl}}, a^{\text{op}}) - \log \pi^{\text{pl}}(a^{\text{pl}} | s) | a^{\text{pl}}] \right] \\
& = \max_{\pi^{\text{pl}}} \mathbb{E}_{a^{\text{pl}} \sim \pi^{\text{pl}}(\cdot | s)} \left[\underbrace{\min_{a^{\text{op}}} Q(s, a^{\text{pl}}, a^{\text{op}}) - \log \pi^{\text{pl}}(a^{\text{pl}} | s)}_{Q^{\text{pl}}(s, a^{\text{pl}})} \right] \\
& = \log \sum_{a^{\text{pl}}} \exp Q^{\text{pl}}(s, a^{\text{pl}}),
\end{aligned}$$

where the second last equality follows choosing a greedy policy π^{op} that selects the opponent action that minimizes the joint quality function $Q(s, a^{\text{pl}}, a^{\text{op}})$.

The last equality is more involved and it is explained in the following lines:

$$\mathbb{E}_{a^{\text{pl}} \sim \pi^{\text{pl}}(\cdot | s)} [Q^{\text{pl}}(s, a^{\text{pl}}) - \log \pi^{\text{pl}}(a^{\text{pl}} | s)] = \sum_{a^{\text{pl}}} \pi^{\text{pl}}(a^{\text{pl}} | s) (Q^{\text{pl}}(s, a^{\text{pl}}) - \log \pi^{\text{pl}}(a^{\text{pl}} | s))$$

The latter expression is a strictly concave with respect to each decision variable $\pi(a|s)$. So if the derivative with respect to each decision variable $\pi^{\text{pl}}(a^{\text{pl}}|s)$ is zero, we have found the desired global maximum. The normalization is imposed once the maximum has been found. Taking the derivative for a particular decision variable, and equating to zero, we have:

$$(Q^{\text{pl}}(s, a^{\text{pl}}) - \log \pi^{\text{pl}}(a^{\text{pl}} | s)) - 1 = 0$$

It follows that:

$$\pi^{\text{pl}}(a | s) \propto \exp Q^{\text{pl}}(s, a^{\text{pl}})$$

and imposing the proper normalization, we obtain the maximizing policy $\pi^{\text{pl},*}$ with the form:

$$\pi^{\text{pl},*}(a^{\text{pl}}|s) = \frac{\exp Q^{\text{pl}}(s, a^{\text{pl}})}{\sum_{a^{\text{pl}}} \exp Q^{\text{pl}}(s, a^{\text{pl}})}$$

Finally, computing the expectation with respect to the maximizing policy:

$$\begin{aligned} & \mathbb{E}_{a^{\text{pl}} \sim \pi^{\text{pl},*}(\cdot|s)} [Q^{\text{pl}}(s, a^{\text{pl}}) - \log \pi^{\text{pl}}(a^{\text{pl}}|s)] \\ &= \sum_{a^{\text{pl}}} \pi^{\text{pl},*}(a^{\text{pl}}|s) (Q^{\text{pl}}(s, a^{\text{pl}}) - \log \pi^{\text{pl},*}(a^{\text{pl}}|s)) \\ &= \sum_{a^{\text{pl}}} \frac{\exp Q^{\text{pl}}(s, a^{\text{pl}})}{\sum_{a^{\text{pl}}} \exp Q^{\text{pl}}(s, a^{\text{pl}})} \left(Q^{\text{pl}}(s, a^{\text{pl}}) - \log \frac{\exp Q^{\text{pl}}(s, a^{\text{pl}})}{\sum_{a^{\text{pl}}} \exp Q^{\text{pl}}(s, a^{\text{pl}})} \right) \\ &= \sum_{a^{\text{pl}}} \frac{\exp Q^{\text{pl}}(s, a^{\text{pl}})}{\sum_{a^{\text{pl}}} \exp Q^{\text{pl}}(s, a^{\text{pl}})} \left(Q^{\text{pl}}(s, a^{\text{pl}}) - Q^{\text{pl}}(s, a^{\text{pl}}) + \log \sum_{a^{\text{pl}}} \exp Q^{\text{pl}}(s, a^{\text{pl}}) \right) \\ &= \sum_{a^{\text{pl}}} \frac{\exp Q^{\text{pl}}(s, a^{\text{pl}})}{\sum_{a^{\text{pl}}} \exp Q^{\text{pl}}(s, a^{\text{pl}})} \left(\log \sum_{a^{\text{pl}}} \exp Q^{\text{pl}}(s, a^{\text{pl}}) \right) \\ &= \log \sum_{a^{\text{pl}}} \exp Q^{\text{pl}}(s, a^{\text{pl}}) \end{aligned} \tag{58}$$

Basically, we have shown that the optimization problem is solved when the player follows a soft-max policy with respect to the quality function $Q^{\text{pl}}(a^{\text{pl}}|s) = \min_{a^{\text{op}}} Q(s, a^{\text{pl}}, a^{\text{op}})$. This explains the steps for the player policy in Algorithm 2. In addition, replacing the definition $Q^{\text{pl}}(a^{\text{pl}}|s) = \min_{a^{\text{op}}} Q(s, a^{\text{pl}}, a^{\text{op}})$ in (58), one gets the saddle point update (12) in Algorithm 2.

We still need to proceed similarly to motivate the opponent policy derivation from the quality function (2). To this end, we maximize with respect to the player before minimizing for the opponent, we have:

$$\begin{aligned} & \min_{\pi^{\text{op}}} \max_{\pi^{\text{pl}}} F(\pi^{\text{pl}}, \pi^{\text{op}}, s) \\ &= \min_{\pi^{\text{op}}} \max_{\pi^{\text{pl}}} \mathbb{E}_{a^{\text{pl}} \sim \pi^{\text{pl}}(\cdot|s), a^{\text{op}} \sim \pi^{\text{op}}(\cdot|s)} [Q(s, a^{\text{pl}}, a^{\text{op}}) - \log \pi^{\text{pl}}(a^{\text{pl}}|s)] \\ &= \min_{\pi^{\text{op}}} \max_{\pi^{\text{pl}}} \mathbb{E}_{a^{\text{op}} \sim \pi^{\text{op}}(\cdot|s)} \left[\mathbb{E}_{a^{\text{pl}} \sim \pi^{\text{pl}}(\cdot|s)} [Q(s, a^{\text{pl}}, a^{\text{op}}) - \log \pi^{\text{pl}}(a^{\text{pl}}|s) | a^{\text{op}}] \right] \\ &= \min_{\pi^{\text{op}}} \mathbb{E}_{a^{\text{op}} \sim \pi^{\text{op}}(\cdot|s)} \left[\max_{\pi^{\text{pl}}} \mathbb{E}_{a^{\text{pl}} \sim \pi^{\text{pl}}(\cdot|s)} [Q(s, a^{\text{pl}}, a^{\text{op}}) - \log \pi^{\text{pl}}(a^{\text{pl}}|s) | a^{\text{op}}] \right] \end{aligned}$$

The innermost maximization is solved again by observing that it is a concave function in the decision variables, normalizing one obtains the maximizer policy, and plugging that in the expectation gives the soft-max function with respect to the player action a^{pl} . We define this function as the quality function of the opponent, because it is the amount of information that can be used by the opponent to decide its move.

$$Q^{\text{op}}(s, a^{\text{op}}) = \log \sum_{a^{\text{pl}}} \exp Q(s, a^{\text{pl}}, a^{\text{op}})$$

It remains to face the external minimization with respect to the opponent policy. This is trivial, the opponent can simply act greedily since it is not regularized :

$$\min_{\pi^{\text{op}}} \mathbb{E}_{a^{\text{op}} \sim \pi^{\text{op}}(\cdot|s)} [Q^{\text{op}}(s, a^{\text{op}})] = \min_{a^{\text{op}}} Q^{\text{op}}(s, a^{\text{op}})$$

This second part clarifies the updates relative to the opponent in Algorithm 2.

Notice that the algorithm iterates in order to obtain a more and more precise estimate of the joint quality function $Q(s, a^{\text{pl}}, a^{\text{op}})$. When it converges, the quality functions for the player and the agent respectively are obtained, thanks to the transformations illustrated here and in the body of Algorithm 2.

F Additional Experimental Results

Additional Gridworlds. The trade-off determined by the parameter α , described in the main paper, is observed for other Gridworlds whose rewards are again linear combinations of the one-hot features associated to each state. The results are reported in Figure 3.

Shifted Plots. When $\epsilon_L \neq 0$, it may be also insightful to report the policy performances as function of the *noise difference* $\epsilon_E - \epsilon_L$, i.e., because this quantity is proportional to the term $\max_{s,a} \|T^{L,\epsilon_L}(\cdot | s, a) - T^{E,\epsilon_E}(\cdot | s, a)\|_1$ ⁹. These plots are reported in Figure 5.

A Simple Exception. The trade-off is not visible in the simplest possible environment where the aim is to find the terminal state. In this situation, the opponent cannot induce detrimental behavior for the agent because all the possible state has the same reward. The opponent cannot lead the agent to a state where it receives a low reward. The results are reported in the first line of Figure 3 as a function of ϵ_E and in Figure 5 as a function of the noise difference $\epsilon_E - \epsilon_L$.

Uncertainty Quantification. In all the plots, the curves’ uncertainty is due to the stochasticity of the recovered policies. We quantified the uncertainty as follows: We compute the average reward of $|\mathcal{S}|$ trajectories such that they all start from a different starting point. Then, we store this average, and we repeat the previous point for another group of $|\mathcal{S}|$ trajectories. We repeated this process for 1000 groups of $|\mathcal{S}|$ trajectories, and we report the uncertainty as the standard deviation of the 1000 averages obtained from each one of the trajectories group.

Low Dimensional Features. In Figure 6, we investigate the effect of our algorithms on a reward described only by three features. In particular, the feature vector associated with a state s is of length 3, and each entry can be either 1 or 0. The first entry is equal to 1 if, in that state, there is the danger of type 1, equal to 0 otherwise. Analogously, the second equals 1 to indicate the danger of type 2, whereas the last feature equals 1 for non-terminal states. The true reward is obtained by taking the inner product of the feature vector of each state, and the true reward weights $\mathbf{w} = [-1, -5, -1]$. Here, w indicates that the danger of type 1 leads to a penalty of -1 ; the danger of type 2 leads to a severe penalty of -5 , and finally, each cell that is not terminal leads to a navigation cost of -1 . The results in this specific environment suggest that our method improves MCE IRL more significantly in the low-dimensional feature case.

Fixed Starting State. Finally, we also confirmed our findings fixing the starting point to be in the furthest possible position of the goal. It can be seen as one of the most challenging starting points since all the grid has to be safely crossed. For this task, we reduced the Adam learning rate to 0.15.

Hyperparameters and Tolerances for Linear Reward Problems. In the settings whose reward is linear in the provided features, we adopted the tolerances described in Table 2 and Adam hyperparameters reported in Table 1.

Objectworld: Neural Network Architecture. The Objectworld non-linear reward has been approximated by a two 2D convolutional layers neural network with the ReLu activation function. The size of both hidden layers is equal to the number of input features constructed, as explained in the main text. The network weights are optimized using Adam with the hyperparameters reported in Table 3.

Finite Horizon Objectworld. ObjectWorld is an environment initially introduced as a finite horizon problem [36]. At the same time, in the main text, we modified it to an infinite horizon problem to apply our algorithm directly. Here we modify our algorithm and benchmark it in a finite horizon Objectworld. In agreement with [36], the positions within three cells to an outer blue object are

⁹Indeed, $\max_{s,a} \|T^{L,\epsilon_L}(\cdot | s, a) - T^{E,\epsilon_E}(\cdot | s, a)\|_1 = |\epsilon_L - \epsilon_E| \max_{s,a} \|T^{\text{ref}}(\cdot | s, a) - \bar{T}(\cdot | s, a)\|_1$. Then, considering that in our experimental setting T^{ref} is deterministic and \bar{T} is uniform, we have: $\max_{s,a} \|T^{\text{ref}}(\cdot | s, a) - \bar{T}(\cdot | s, a)\|_1 = 2 \left(1 - \frac{1}{|\mathcal{S}|}\right)$. Hence, the following holds: $\max_{s,a} \|T^{L,\epsilon_L}(\cdot | s, a) - T^{E,\epsilon_E}(\cdot | s, a)\|_1 = 2 \left(1 - \frac{1}{|\mathcal{S}|}\right) |\epsilon_L - \epsilon_E|$.

assigned a reward equal to -1 , but if they are also within two cells from an outer green object, the reward is $+1$. All other positions are assigned a null reward, so the presence of objects with other colors is not relevant in determining the reward function. In the finite horizon setting, we evaluate a policy's performance via the reward accumulated along a trajectory of length $2N$, where N is the Objectworld side dimension. Hence, the optimal policy attempts to the areas with positive rewards and stays there until the end of the maximum trajectory length. It is thus essential to add the "stay" action to the action space of the agent.

In order to adapt our algorithm to the finite horizon setting, we used Algorithm 3 from [37] (instead of the infinite horizon policy propagation proposed in [31, Section V.C]) to compute the state visitation frequency at a fixed horizon. A proof of concept of our algorithm on a 10×10 Objectworld is given in Figure 7. The neural network used to approximate the reward function consists of two 2D convolutional layers with the ReLu activation function. The size of both hidden layers is equal to the number of input features constructed as originally proposed in [36]. We adopted Adam [35] as an optimizer with hyperparameters in Table 4. Finally, as done in [36], we consider the optimal policy as the expert rather than the soft-optimal one. As far as the features available to the learner are considered, we adopted the discrete features proposed in the previous work using this benchmark.

Table 1: Reward optimizer hyperparameters

Hyperparameter	Value
IRL Optimizer	Adam
Learning rate	0.5
Weight decay	0.0
First moment exponential decay rate	0.9
Second moment exponential decay rate	0.99
Numerical stabilizer	$1e - 7$
Number of steps	200

Table 2: MDP solver parameters

Parameter	Value
2 Player soft value iteration tolerance	$1e - 10$
Soft value iteration tolerance	$1e - 10$
Value iteration tolerance	$1e - 10$
Policy propagation tolerance	$1e - 10$

Table 3: Infinite horizon Objectworld reward optimizer hyperparameters

Hyperparameter	Value
IRL Optimizer	Adam
Learning rate	$1e - 3$
Weight decay	0.01
First moment exponential decay rate	0.9
Second moment exponential decay rate	0.999
Numerical stabilizer	$1e - 8$
Number of steps	200

Table 4: Finite horizon Objectworld reward optimizer hyperparameters

Hyperparameter	Value
IRL Optimizer	Adam
Learning rate	$1e - 3$
Weight decay	0.05
First moment exponential decay rate	0.9
Second moment exponential decay rate	0.999
Numerical stabilizer	$1e - 8$
Number of steps	200

GridWorlds: Performance as a function of Expert Noise

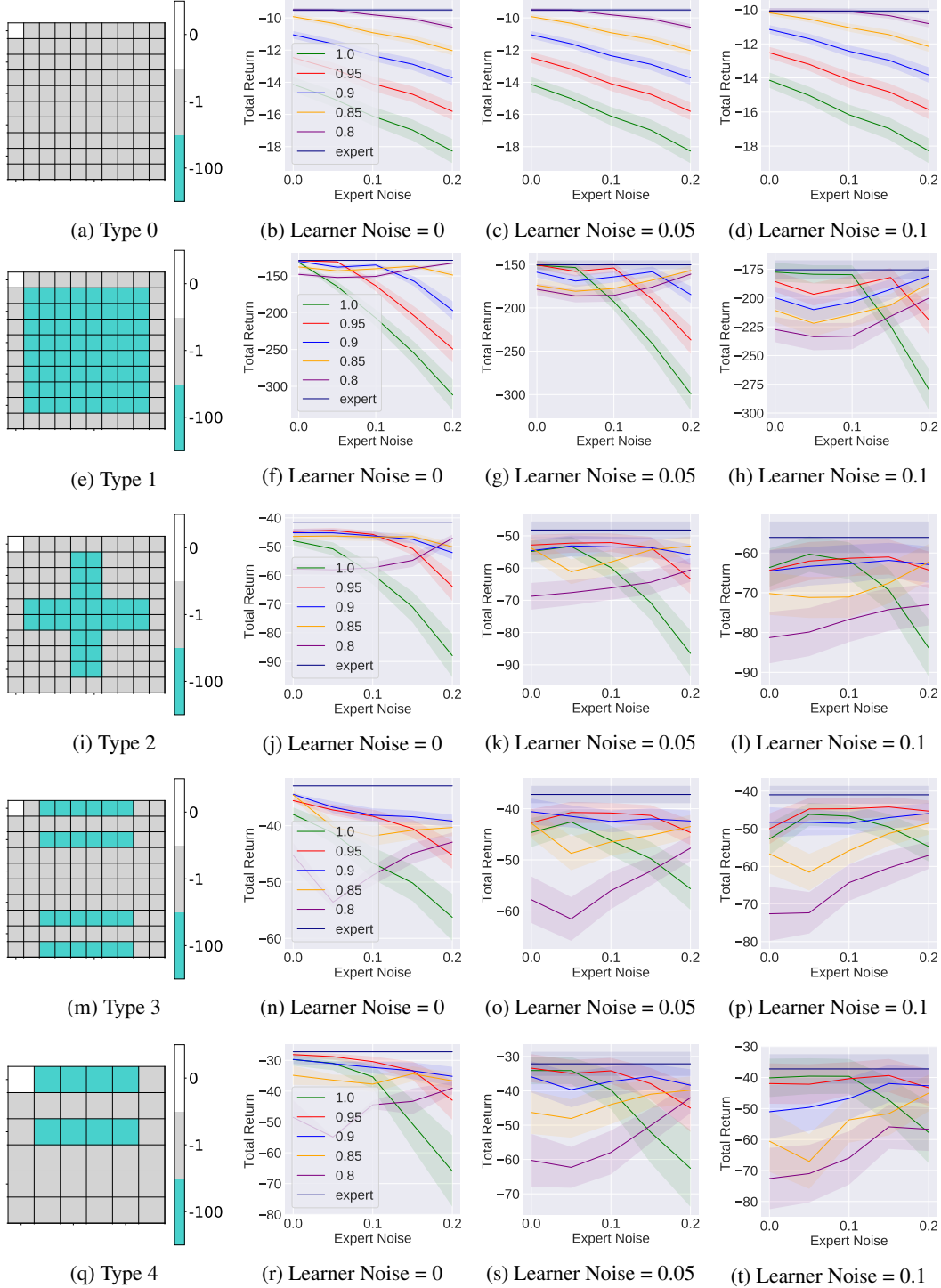


Figure 3: On the x-axis, we report different expert noises ϵ_E , while the y-axis indicates the total expected return for the policy that is recovered from the expert acting in $M_{\theta^*}^{E, \epsilon_E}$ varying α . All the recovered policies are evaluated on the learner MDP endowed with the true reward $M_{\theta^*}^{L, \epsilon_L}$. The expert baseline in the plots is the policy obtained in $M_{\theta^*}^{L, \epsilon_L}$ applying Value-Iteration. We decided to adopt a uniform \bar{T} in defining $M_{\theta^*}^{E, \epsilon_E}$ and $M_{\theta^*}^{L, \epsilon_L}$, and we tested all the possible pairs picking ϵ_L from the set $\{0.0, 0.05, 0.1\}$ and ϵ_E from $\{0.0, 0.05, 0.1, 0.15, 0.2\}$. Each row of the Figure reports starting from left to right the environment reward and then the results for a learner noise ϵ_L respectively equal to 0.0, 0.05, and 0.1.

Fixed Starting State at the bottom right cell: Learner Noise = 0

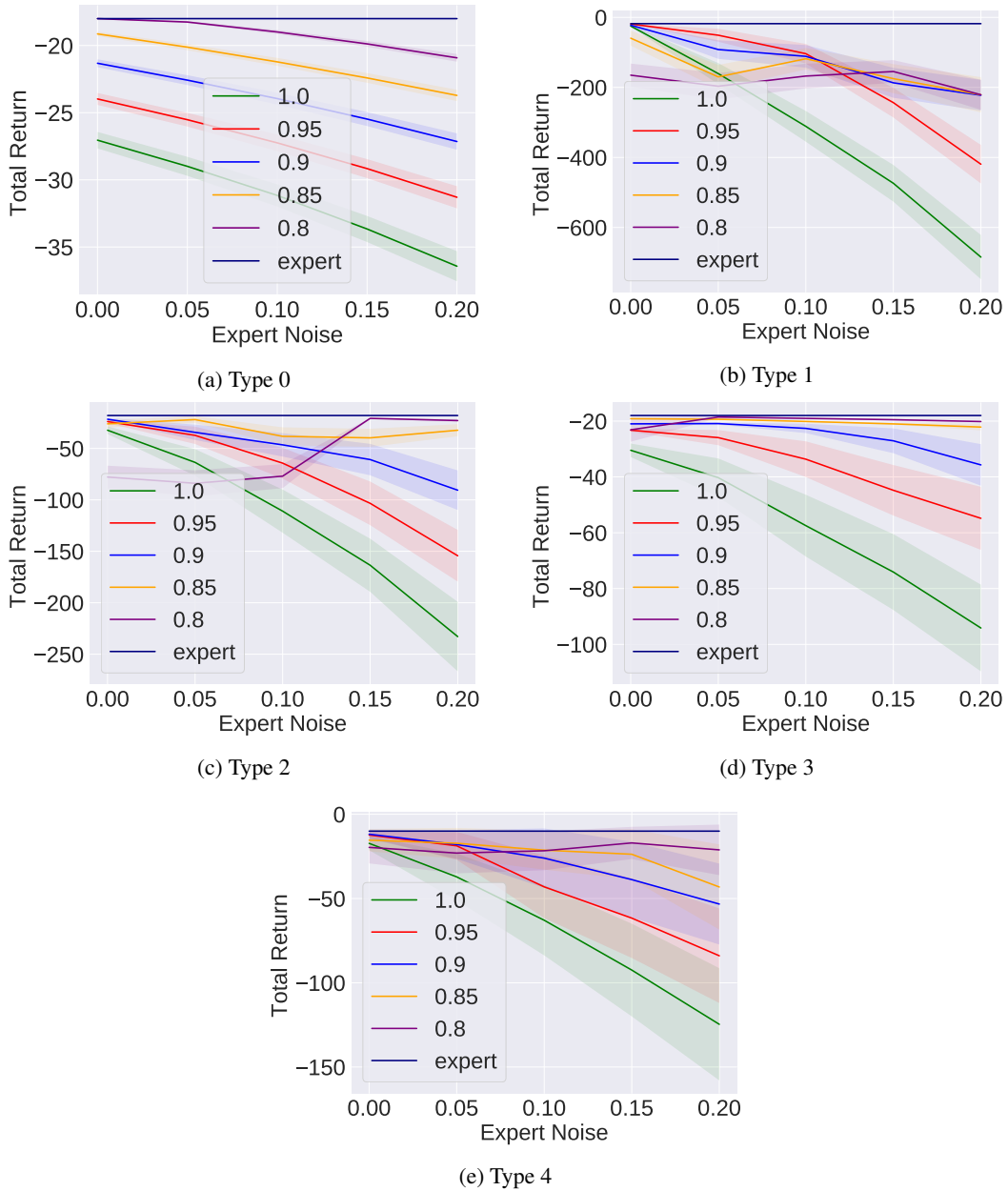


Figure 4: This Figure reports, instead, the total expected return obtained fixing the starting state on the corner opposite to the goal corner. The label Type refers to the corresponding environments of Figures 3 and 5. The trade-off determined by α is particularly evident for environment Type 2, Type 3, and Type 4, while again Type 0 is an exception.

GridWorlds: Performance as a function of Noise Difference

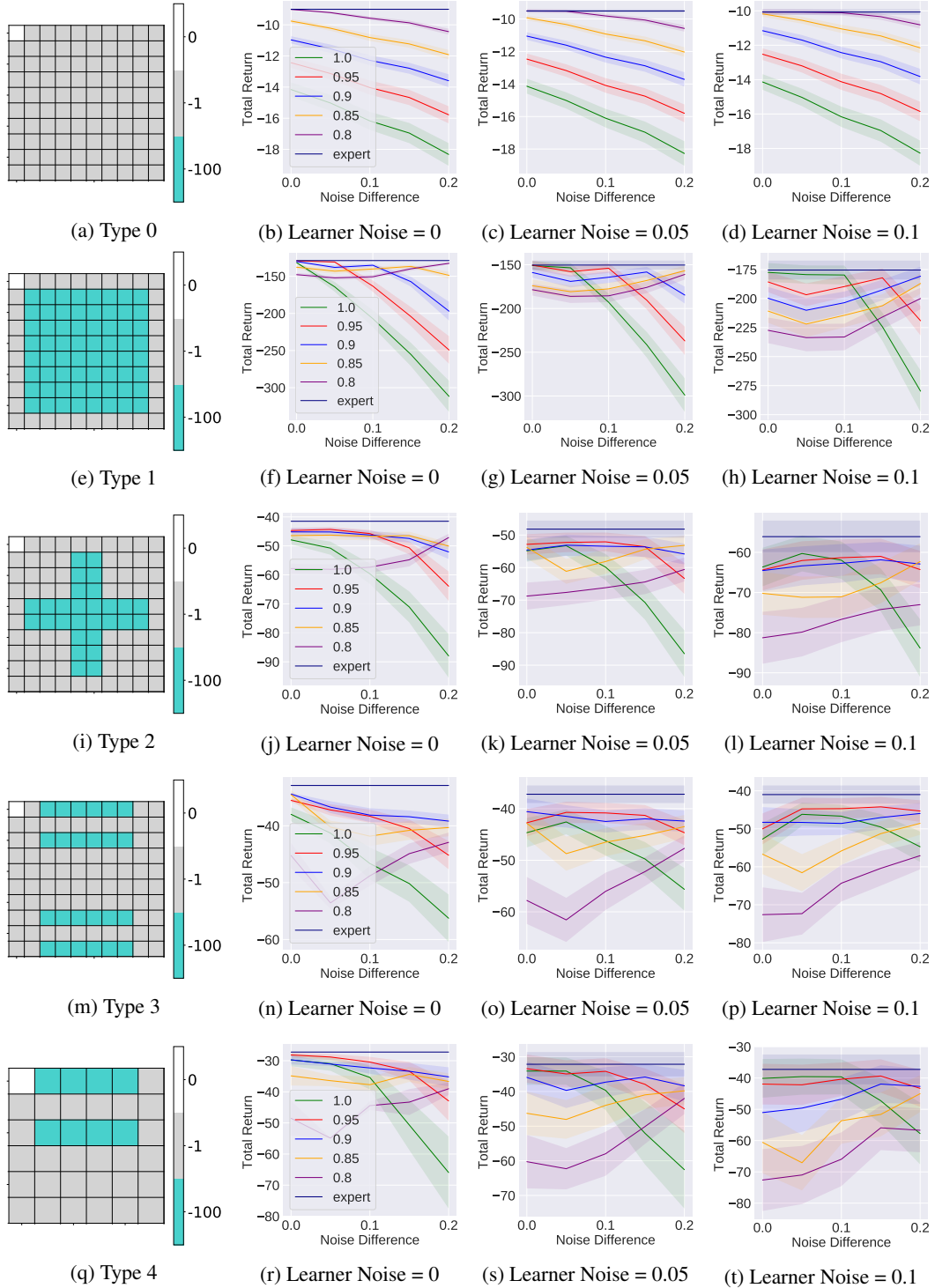


Figure 5: The Figure above shows the same results already presented in Figure 3 but shifting the x-axis in order to represent similar behavior of the curves as a function of the noise difference $\epsilon_E - \epsilon_L$.

Low Dimensional Features

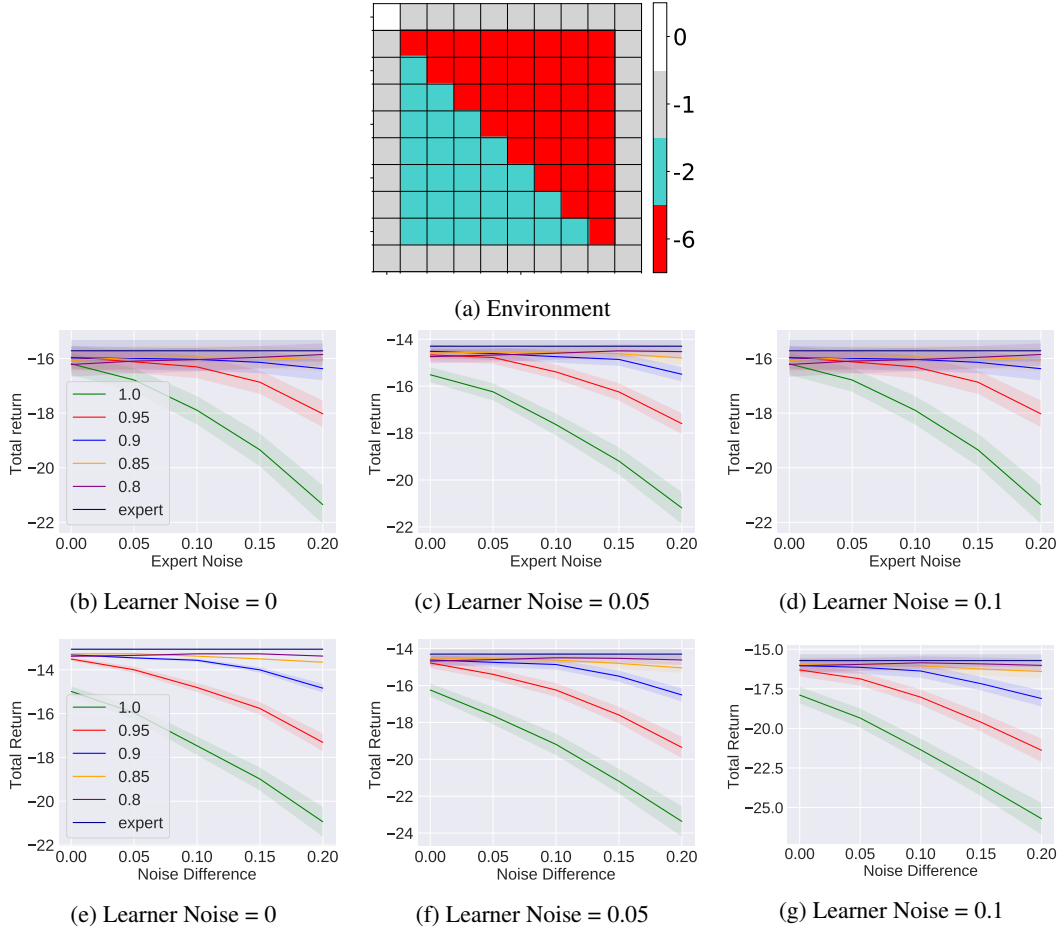
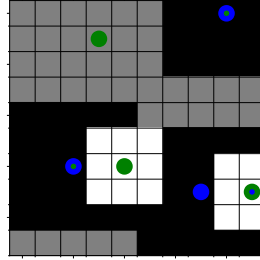
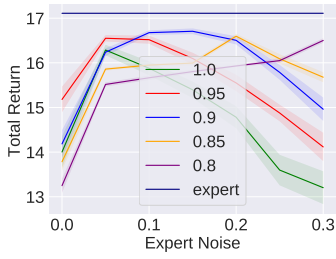


Figure 6: The Figure reports the results of our algorithm in the case of Low Dimensional Features. In particular, in the first line, 6a shows the reward map of the environment, 6b, 6c, and 6d the results expressed as a function of the expert noise ϵ_E on the x-axis while 6e, 6f, and 6g show the same results as a function of the noise difference $\epsilon_E - \epsilon_L$.

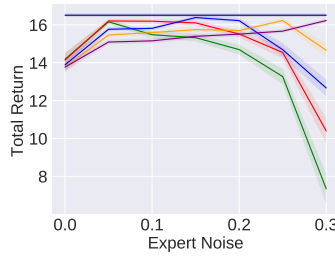
Finite Horizon ObjectWorld



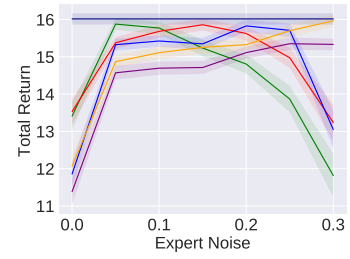
(a) Environment



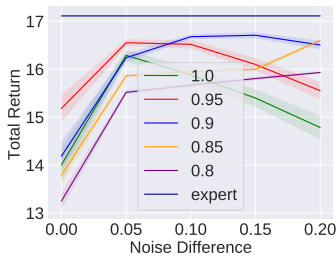
(b) Learner Noise = 0



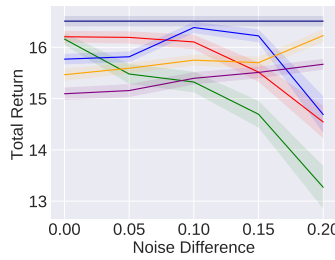
(c) Learner Noise = 0.05



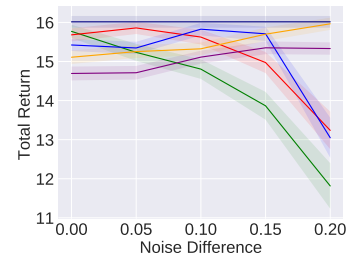
(d) Learner Noise = 0.1



(e) Learner Noise = 0



(f) Learner Noise = 0.05



(g) Learner Noise = 0.1

Figure 7: The Figure reports the results of our algorithm in the case of Finite Horizon ObjectWorld. In particular, in the first line, 7a shows the reward map of the environment, 7b, 7c, and 7d the results expressed as a function of the expert noise ϵ_E on the x-axis while 7e, 7f, and 7g show the same results as a function of the noise difference $\epsilon_E - \epsilon_L$.